6. Full-face heading

6.1 Urban railway tunnel underneath the Stuttgart airport runway, Germany

6.1.1 Introduction

The urban railway of Stuttgart, Germany, was extended in 2001 by a section starting at the Airport station and running underneath the airport area to the city of Filderstadt-Bernhausen. The Airport station (construction lot 72) and a continuation of limited extent towards Bernhausen (lot 92) were constructed by the cut-and-cover method. A 2.15 km long tunnel section driven by underground construction (lot 601) follows. It undercrosses among other areas the apron and the runway of the airport. The approx. 500 m long tunnel section of the Filderstadt-Bernhausen station (lot 602) was constructed by the cut-and-cover method (Fig. 6.1).

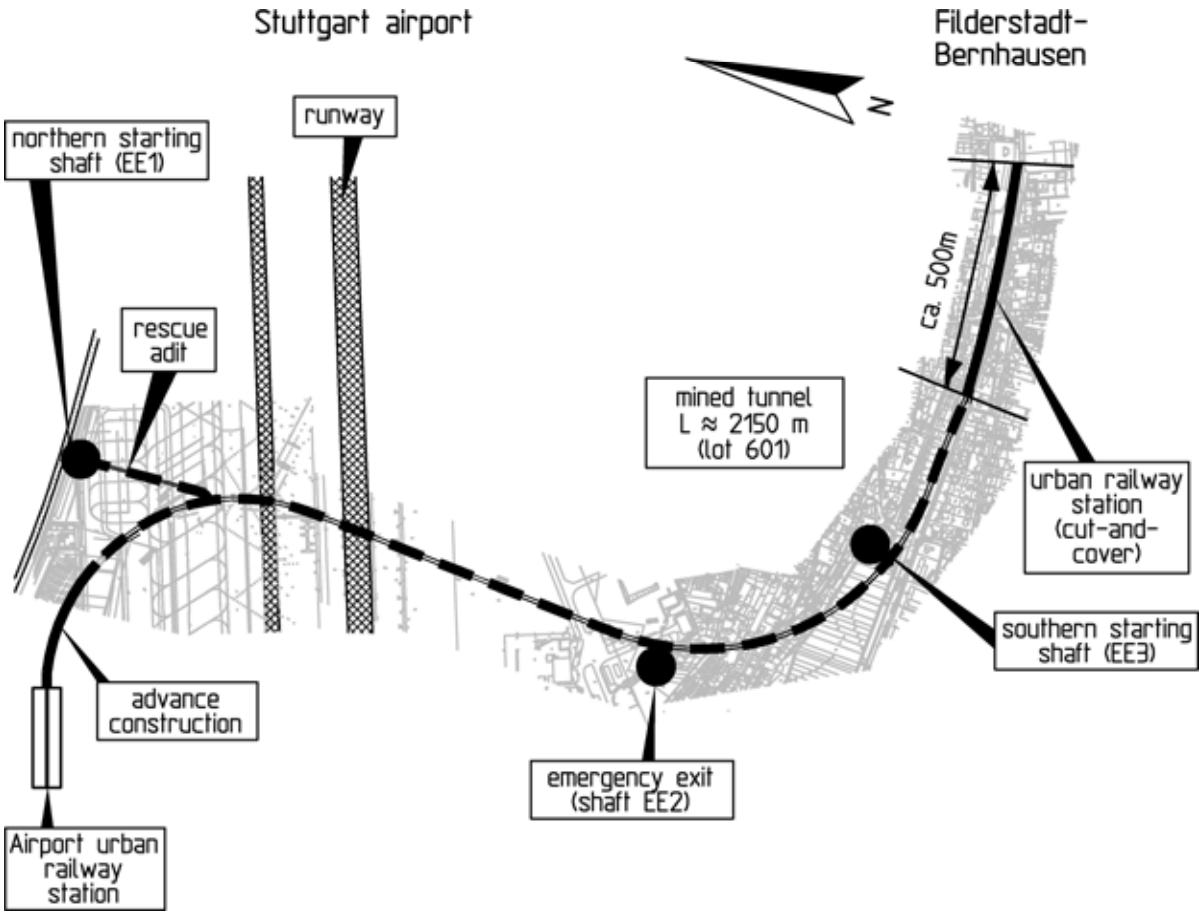

Fig. 6.1: Undercrossing of Stuttgart airport, site plan

The present Chapter describes the tunnel section of lot 601 driven by underground construction, with an emphasis on the undercrossing of the runway of the airport. In this section the absolute and

differential ground surface subsidence due to the tunneling had to be kept as small as possible. This task proved to be quite demanding, because settlement-sensitive, soft valley deposits and fill are locally encountered in the runway area and the groundwater table lies above the tunnel roof. Lowering the groundwater table during tunneling could therefore not be permitted, because of the risk of large settlements. The shotcrete support had thus to be constructed with a low water permeability and designed to withstand the water pressure. For the design of the shotcrete membrane it had further to be taken into account that high horizontal stresses exist especially in the mudstones of the Lias α formation, in which the major part of the mined tunnel section is located (see Chapter 4.1).

6.1.2 Structure

The course of the alignment and the ground profile are shown in Fig. 6.2. Following lot 92, the alignment descends in the direction of Bernhausen up to the area in front of the runway.

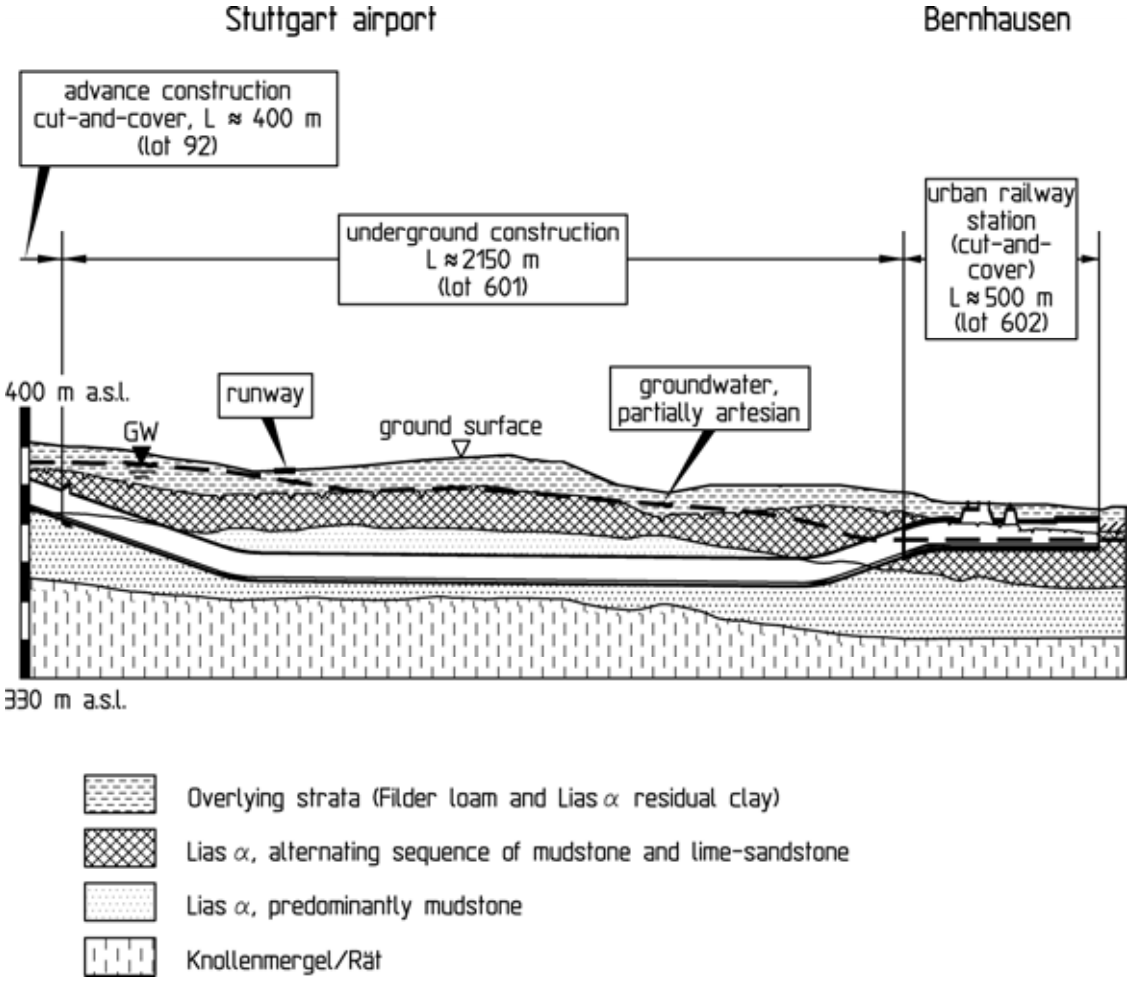

Fig. 6.2: Undercrossing of Stuttgart airport, longitudinal section with ground profile

The tunnel then runs horizontally over a length of approx. 1400 m (lot 601). The following gradient extends into the cut-and-cover section (lot 602). In the area of the station the alignment then runs approximately horizontally again.

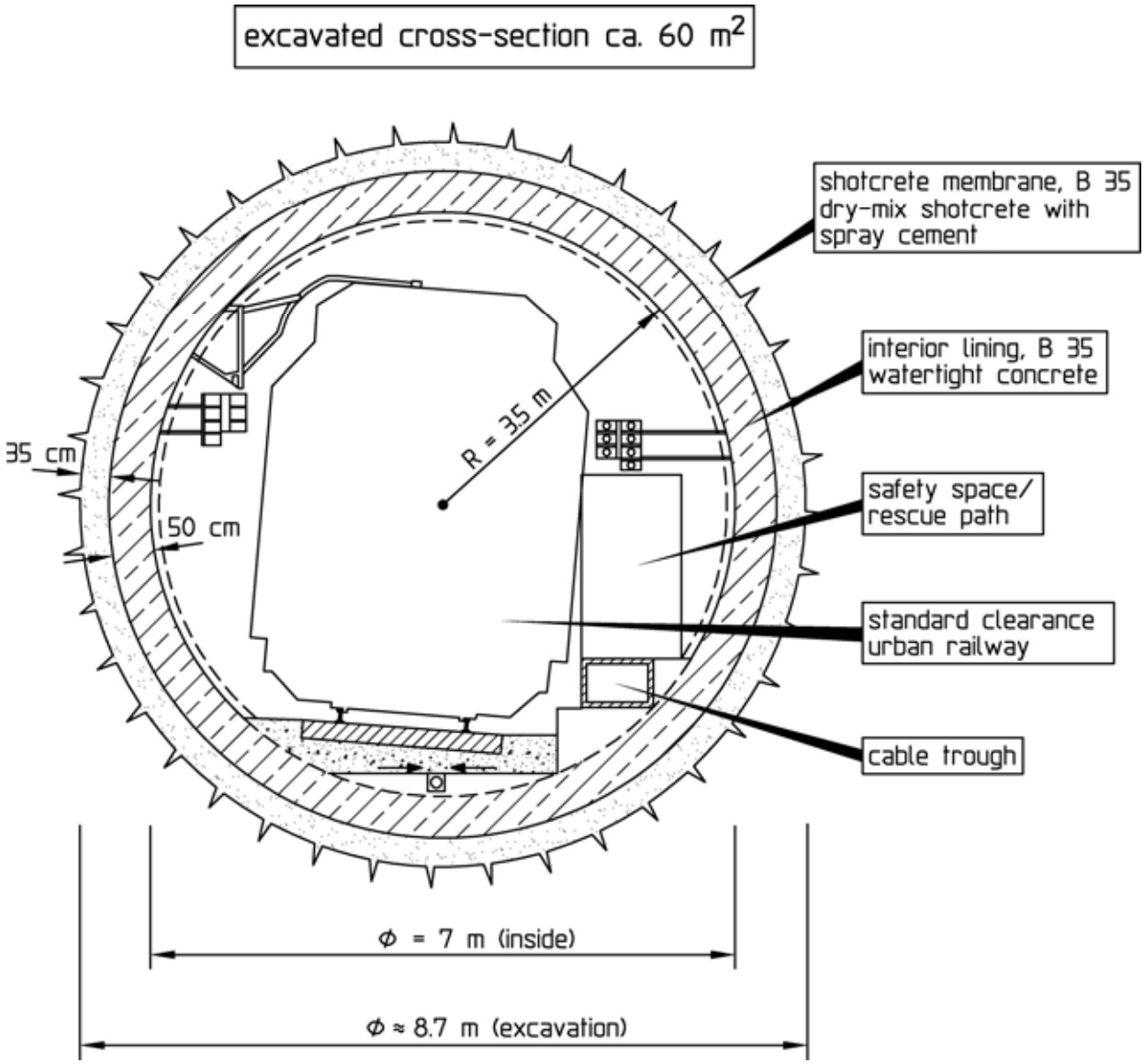

Fig. 6.3: Single-tracked tunnel tube, standard profile

Two single-tracked tunnel tubes are planned for the mined tunnel section (lot 601), only one of which has been built for the time being, however. The tunnel tube was constructed with a circular profile, among other reasons also in order to be able to design the shotcrete membrane for the full water pressure. The 30 to 35 cm thick shotcrete membrane was made from alkali-free dry-mix shotcrete with a low water permeability using spray cement as a bonding agent (see Chapter 2.1.2). The excavated diameter is ap-

prox. 8.7 m, the inside diameter 7.0 m. The excavated cross-section of one tunnel tube amounts to approx. 60 m^2 (Fig. 6.3).

In the area of the airport runway the tunnel roof is located approx. 21 m below the ground surface (Fig. 6.4). Stuttgart Airport Co. (Flughafen Stuttgart GmbH, FSG) demanded that the tunneling-induced subsidence in this area has to be limited to 15 mm and the differential subsidence at the ground surface to 1 $^{o}/_{oo}$.

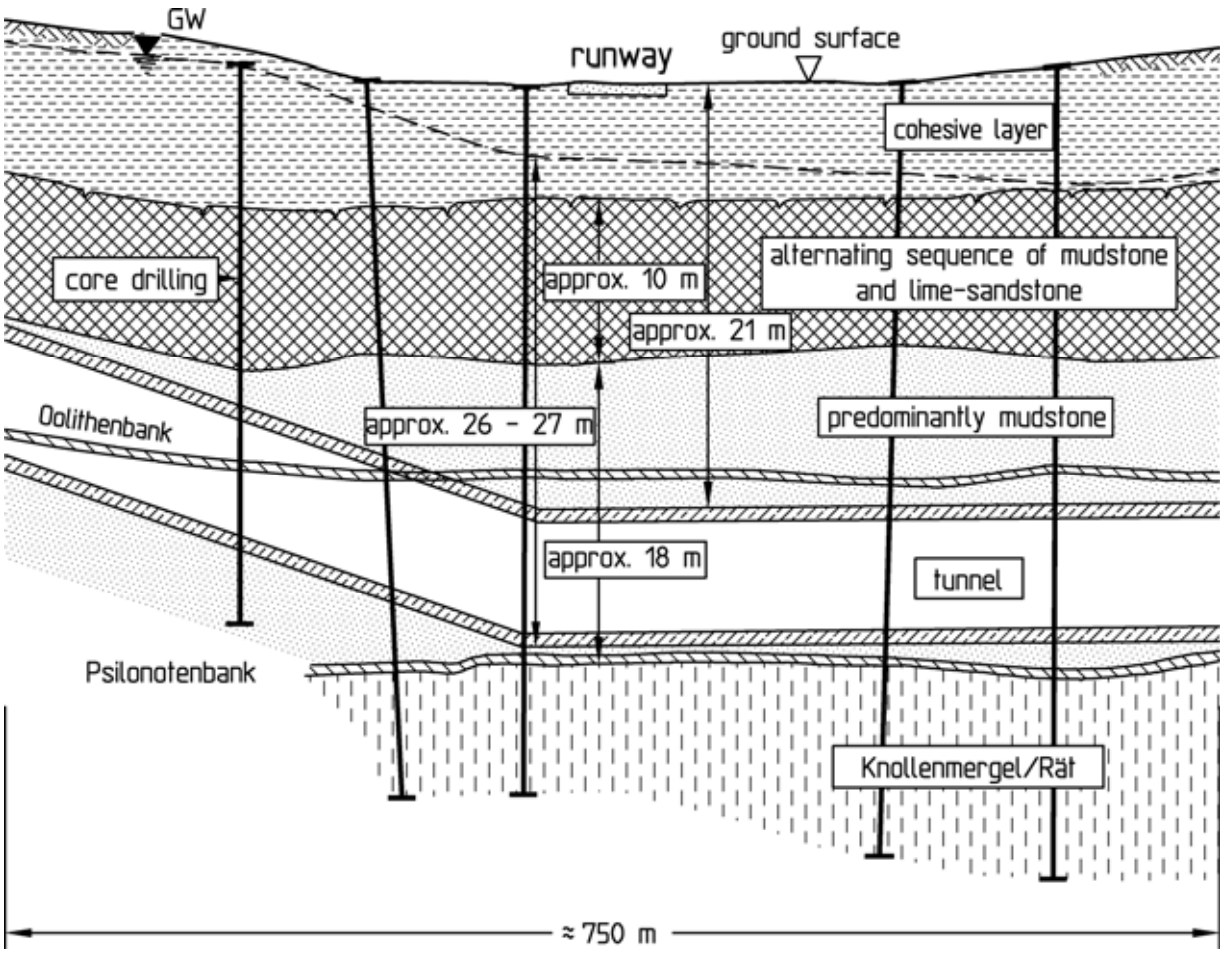

Fig. 6.4: Undercrossing of the runway of Stuttgart airport, longitudinal section with ground profile

6.1.3 Ground and groundwater conditions

The ground profile in the area of the mined tunnel of lot 601 is similar to the one in the area of the Österfeld Tunnel (see Chapter 4.1). The stratigraphic sequence includes the layers of the Knollenmergel, the Rät, the Lias α and the Quarternary (see Fig. 4.4).

According to geotechnical criteria the ground can be subdivided as follows from bottom up (Fig. 4.4, 6.2 and 6.4):

- Knollenmergel and Rät,

- Lias α, predominantly mudstone with single layers of lime-sandstone,

- Lias α, alternating sequence of mudstone and lime-sandstone,

- overlying strata consisting of Lias α residual clay and Filder loam.

To explore the ground and the groundwater conditions core drillings were sunk along the tunnel alignment. Some of these boreholes were equipped as observation wells.

Fig. 6.5: Photograph of the tunnel face showing the transition from the alternating sequence of mudstone and lime-sandstone to the layers consisting predominantly of mudstone

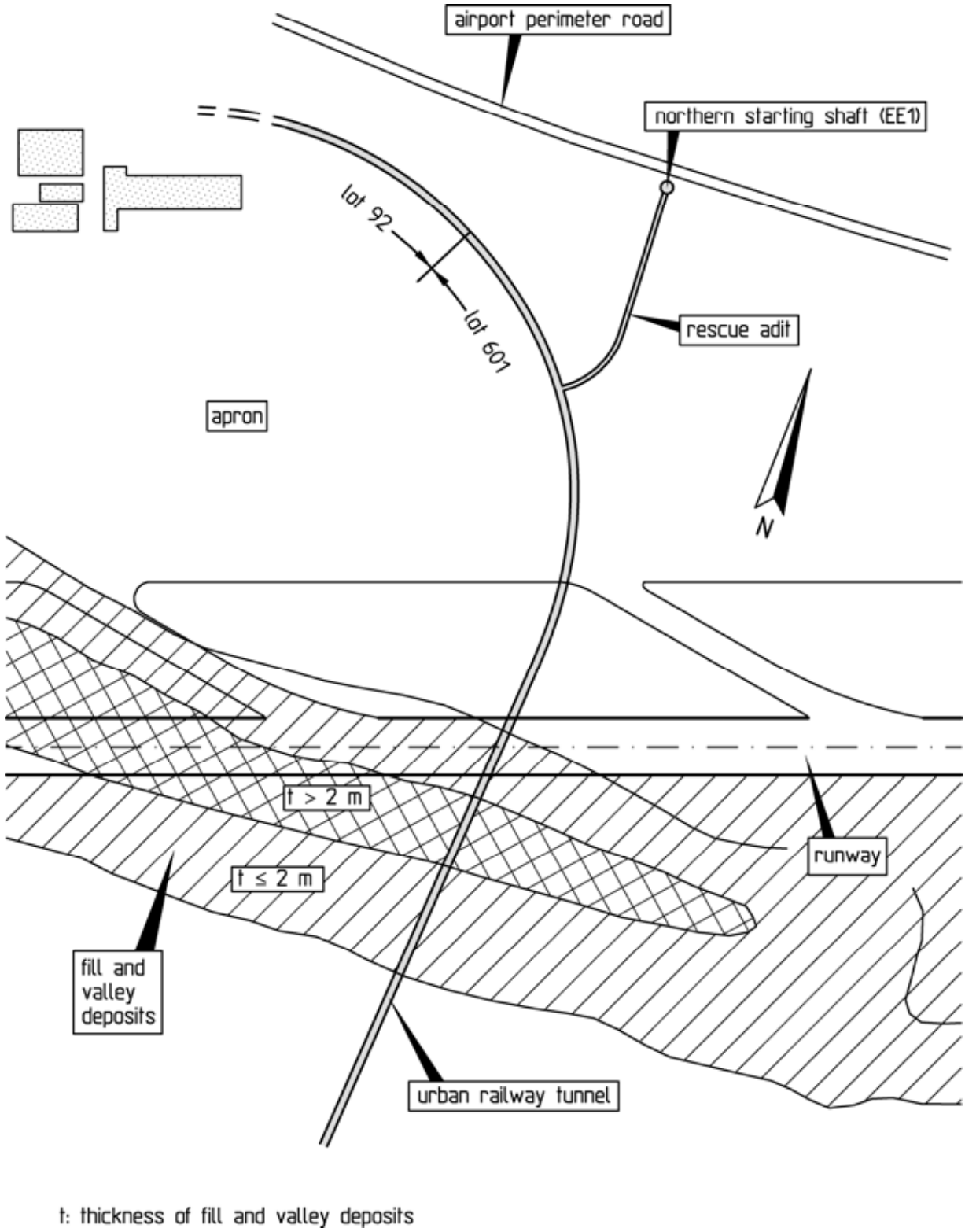

Fig. 6.6: Fill and valley deposits in the runway area of Stuttgart airport

According to the exploration results, the mined tunnel of lot 601 is located over its entire length in the rock layers of the Lias α

formation (Fig. 6.2 and 6.4). In the area of the airport runway it lies completely within the layers consisting predominantly of mudstone. Adjacent to the cut-and-cover tunnel sections, i. e. in the areas with descending or climbing alignment, the tunnel crosses through the alternating sequence of mudstone and banks of lime-sandstone (Fig. 6.2). Fig. 6.5 is a photograph of the temporary tunnel face, in which the lowest banks of lime-sandstone of the alternating sequence, which are also referred to as "main sandstone", are clearly recognizable.

The runway of the airport is founded on cohesive layers (Fig. 6.4) consisting mainly of Filder loam and Lias α residual clay. To the west of the urban railway alignment a lake was formerly located in the area of today's runway, flowing out into a creek running towards the east. In the course of the construction of Stuttgart airport, the area of the lake and the creek was filled up. The existing partially soft and settlement-sensitive valley deposits remained under the fill in the process. The fill and the valley deposits are locally several meters thick (Fig. 6.6).

Fig. 6.7 shows the structural model (see Chapter 2.5.1) derived for the ground in the area of the tunnel section driven by underground construction. The discontinuity fabric is characterized by an orthogonal system of horizontal bedding parallel discontinuities and steep to vertically dipping joints. Unlike to the banks of lime-sandstone, the bedding parallel discontinuities and joints in the mudstone layers are mostly closed or filled with clay and only vaguely recognizable. In the mudstones of the Rät and the Knollenmergel slickensides exist, dipping at 20 to 40° and striking in all directions (see Chapter 4.1.3).

The soil and rock mechanical parameters given in Table 6.1 were specified on the basis of the results of laboratory and in-situ tests as well as experience gained from projects in comparable ground conditions (see Chapter 4.1). For the rock layers of the Lias α formation encountered in the area of the mined tunnel, a transversely isotropic elastic stress-strain behavior, described by 5 independent elastic constants (Wittke, 2000), was assumed for loading below the strength. A further characteristic of the Lias α layers are the low shear strengths on the bedding parallel discontinuities and the joints.

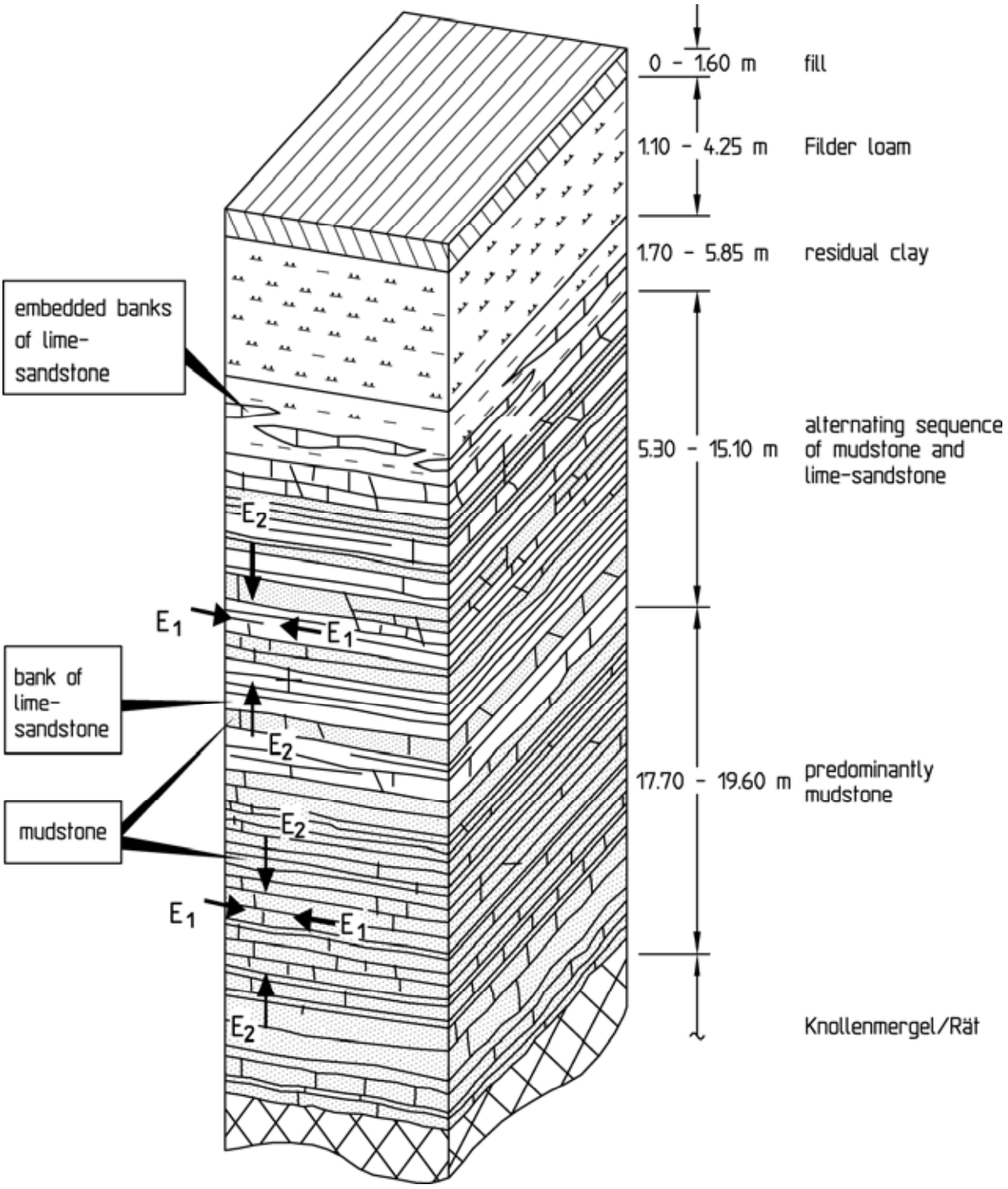

Fig. 6.7: Structural model of the ground in the area of the mined tunnel section (lot 601)

The parameters given in Table 6.1 should be interpreted as characteristic parameters according to DIN 4020 (1990) and were taken as a basis for the stability analyses of the mined tunnel.

Layer	Deformability	Strength	Permeability
Overlying strata	$E = 15$ MN/m^2 $\nu = 0.4$	$\varphi' = 25°$ $c' = 25$ kN/m^2	$k_f \leq 10^{-8}$ m/s
Alternating sequence of mudstone and lime-sandstone	$E_1 = 1500$ MN/m^2 $E_2 = 750$ MN/m^2 $G_2 = 200$ MN/m^2 $\nu_1 = 0.25$ $\nu_2 = 0.2$	Bedding B: $\varphi_B = 20°$ $c_B = 80$ kN/m^2 Joints J1, J2: $\varphi_J = 35°$ $c_J = 40$ kN/m^2	Horizontally: $k_{fH} = 5 \cdot 10^{-5}$ m/s Vertically: $k_{fV} = 10^{-6}$ m/s
Mudstone with single layers of lime-sandstone	$E_1 = 1000$ MN/m^2 $E_2 = 500$ MN/m^2 $G_2 = 200$ MN/m^2 $\nu_1 = 0.25$ $\nu_2 = 0.2$	Bedding B: $\varphi_B = 20°$, $c_B = 0$ Joints J1, J2: $\varphi_J = 35°$, $c_J = 0$	$k_f = 10^{-7}$ m/s
Rät and leached zone of the Knollenmergel	$E = 150$ MN/m^2 $\nu = 0.3$	Discontinuities: $\varphi_D = 17.5°$ $c_D = 10$ kN/m^2	$k_f = 5 \cdot 10^{-7}$ m/s
Knollenmergel, unweathered	$E = 1000$ MN/m^2 $\nu = 0.25$	Slickensides: $\varphi_S = 17.5°$ $c_S = 10$ kN/m^2	$k_f \leq 10^{-8}$ m/s

Table 6.1: Characteristic soil and rock mechanical parameters

The results of in-situ tests and measurements on different structures in the area of Stuttgart have shown that increased horizontal in-situ stresses exist in the Lias α (Grüter, 1988; Wittke, 1990; Wittke, 1991). According to these results, in addition to the horizontal stresses resulting from the dead weight, horizontal stresses of $\Delta\sigma_H = 1$ to 2 MN/m^2 exist in the unweathered mudstone layers and horizontal stresses of $\Delta\sigma_H = 0.5$ to 1.0 MN/m^2 exist in the alternating sequence (Böttcher et al., 1998). The magnitude of these stresses was confirmed by the results of the stress measurements by the overcoring method (Kiehl and Pahl, 1990) carried out in the course of the project presented here. Horizontal in-situ

stresses of $\Delta\sigma_H$ = 0.5 to 1.7 MN/m^2 were derived from the results of these stress measurements.

The permeability tests carried out as part of the exploration showed that the mudstone layers have a much lower water permeability than the lime-sandstone banks. Accordingly, the alternating sequence is inhomogeneous with respect to its permeability. However, since the tunnel diameter is large compared to the thicknesses and the spacing of the layers of the alternating sequence, the alternating sequence can be overall considered approximately homogeneous, if the different permeabilities of the layers is taken into account by introducing an anisotropy (Wittke, 2000). The horizontal permeability of $k_{fH} = 5 \cdot 10^{-5}$ m/s is determined here by the banks of lime-sandstone, whereas the vertical permeability of $k_{fV} = 10^{-6}$ m/s is due to the mudstone (Table 6.1).

The overlying strata, the Lias α layers consisting predominantly of mudstone, the Rät and the Knollenmergel have a much smaller water permeability than the alternating sequence (Table 6.1).

In the northern part of the airport the groundwater of the alternating sequence is mostly artesian. The water table is encountered within the overlying strata (see Fig. 6.2 and 6.4). In the adjacent section up to the southern limit of the airport the groundwater table lies within the alternating sequence. A further section with locally artesian groundwater follows (see Fig. 6.2).

The mined tunnel section of lot 601 is thus located almost over its entire length completely underneath the groundwater table. The maximum height of the water table above the tunnel's invert is reached in the area of the airport runway with approx. 26 to 27 m (see Fig. 6.4).

6.1.4 Fundamentals of the design

During the cut-and-cover construction of the first 400 m of the tunnel (lot 92) the groundwater was lowered to below the construction pit's invert using drawdown wells. Measurements of the groundwater level in the airport and specially in the runway area showed that the drawdown cone had a range of approx. 450 m (Fig. 6.8). To avoid subsidence in the airport area, it became necessary to recharge the groundwater using injection wells (Erichsen and Tegelkamp, 1998).

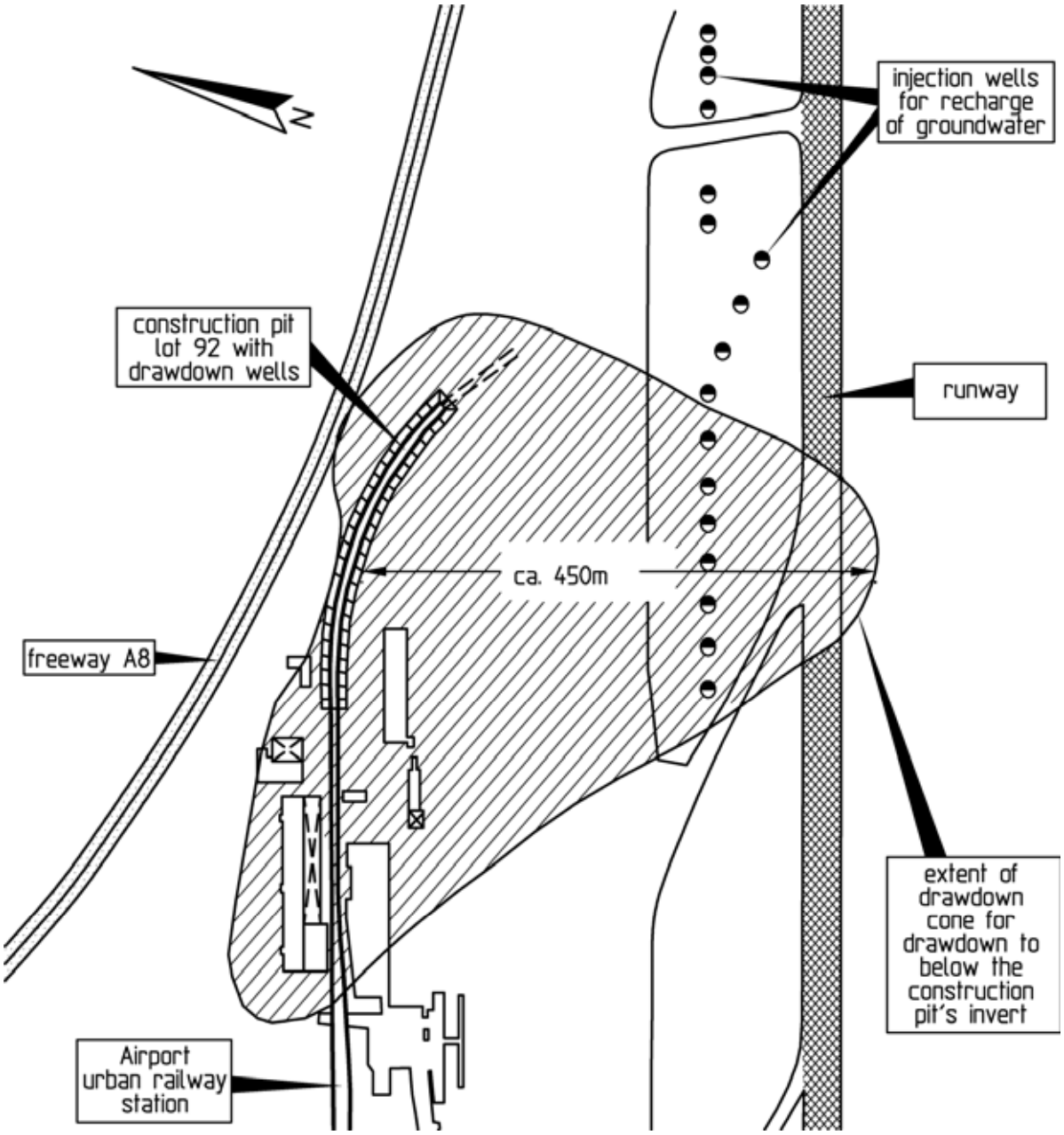

Fig. 6.8: Advance construction (lot 92), site plan with drawdown cone

Especially the soft valley deposits in the runway area (see Fig. 6.6) are very sensitive to settlements. Especially here, but also in other areas, a lowering of the groundwater table as a consequence of the tunnel heading would lead to subsidence due to loss of the hydrostatic uplift. The FSG therefore demanded that no groundwater lowering must occur during the underground tunneling.

Three-dimensional, transient seepage flow analyses were therefore carried out by WBI in the early stages of the project to investigate the influence of the tunnel heading on the groundwater condi-

tions. The program system used for this purpose was developed by WBI (Erichsen, 1994). It is described in detail in Wittke (2000). The assumptions made and the results of the analyses are described and explained in detail in Wittke (2000) as well, and also in Wittke-Gattermann and Wittke (1997). The permeability of the layers consisting predominantly of mudstone (see Chapter 6.1.3), in which the tunnel is located in the area of the undercrossing of the airport runway, as well as the permeability of the shotcrete membrane of the tunnel were varied in the analyses.

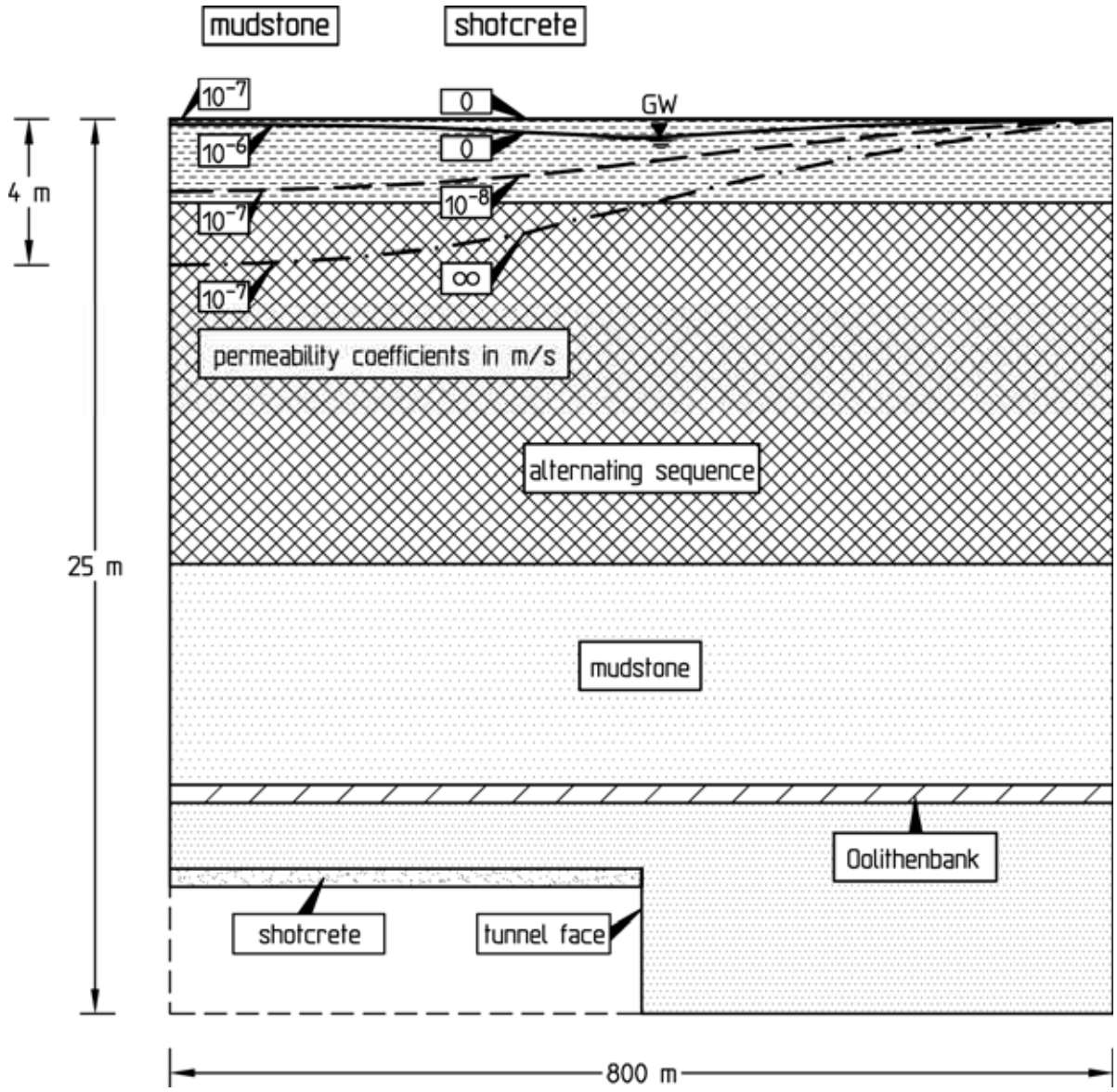

Fig. 6.9: Analyzed drawdown curves of the groundwater table due to the heading, steady state, vertical section through the tunnel axis

Fig. 6.9 shows the drawdown of the groundwater table determined for the steady state in a vertical section through the tunnel axis. For a low permeability of the mudstone layers of $k_f = 10^{-7}$ m/s and an impermeable shotcrete membrane, the groundwater drawdown of < 5 cm can be neglected. An increase in the permeability of the mudstone to $k_f = 10^{-6}$ m/s already leads to a groundwater drawdown of 0.5 m. An increased permeability of the shotcrete membrane yields a considerably increased groundwater drawdown even for a value of k_f of 10^{-7} m/s for the mudstone. The steady state is always reached within a period of time which is short in relation to the construction time (Wittke-Gattermann and Wittke, 1997; Wittke, 2000; Tegelkamp et al., 2000).

Corresponding to the results of the groundwater modeling analyses and to the demand by FSG that groundwater lowering must not occur during the construction of the tunnel, the tunnel had to be supported during the heading by a shotcrete membrane with a low water permeability. The membrane had to be designed to withstand the water pressure. An alkali-free dry-mix shotcrete with spray cement as bonding agent was used. A statically favorable circular profile was selected for the tunnel's cross-section (see Fig. 6.3). The water pressure taken into account as well as the loads resulting from the rock mass pressure, which are essentially determined by the increased horizontal in-situ stresses in the mudstone layers, lead to a required thickness of the reinforced shotcrete membrane of 30 to 35 cm.

An advancing crown excavation was not a reasonable option under the given conditions, because on the one hand an open invert over great lengths could not be permitted since this would lead to a groundwater lowering, and on the other hand a watertight support of the temporary crown invert could not be designed to withstand the water pressure with economically justifiable expense. A full-face heading with a stepped tunnel face was therefore provided for in order to achieve as soon as possible a circular cross-section with closed invert. This was important for statical reasons as well as under the aspect of watertightness, since this design enables water to enter during the tunneling only through the temporary tunnel face and thus only through a comparatively small cross sectional area. This design was also taken as a basis for the three-dimensional seepage flow analyses.

6.1.5 Excavation and support

Fig. 6.10 shows the sequence of excavation and means of support specified for the tunnel heading in the layers consisting predominantly of mudstone. The full-face excavation was subdivided into crown and bench/invert excavation.

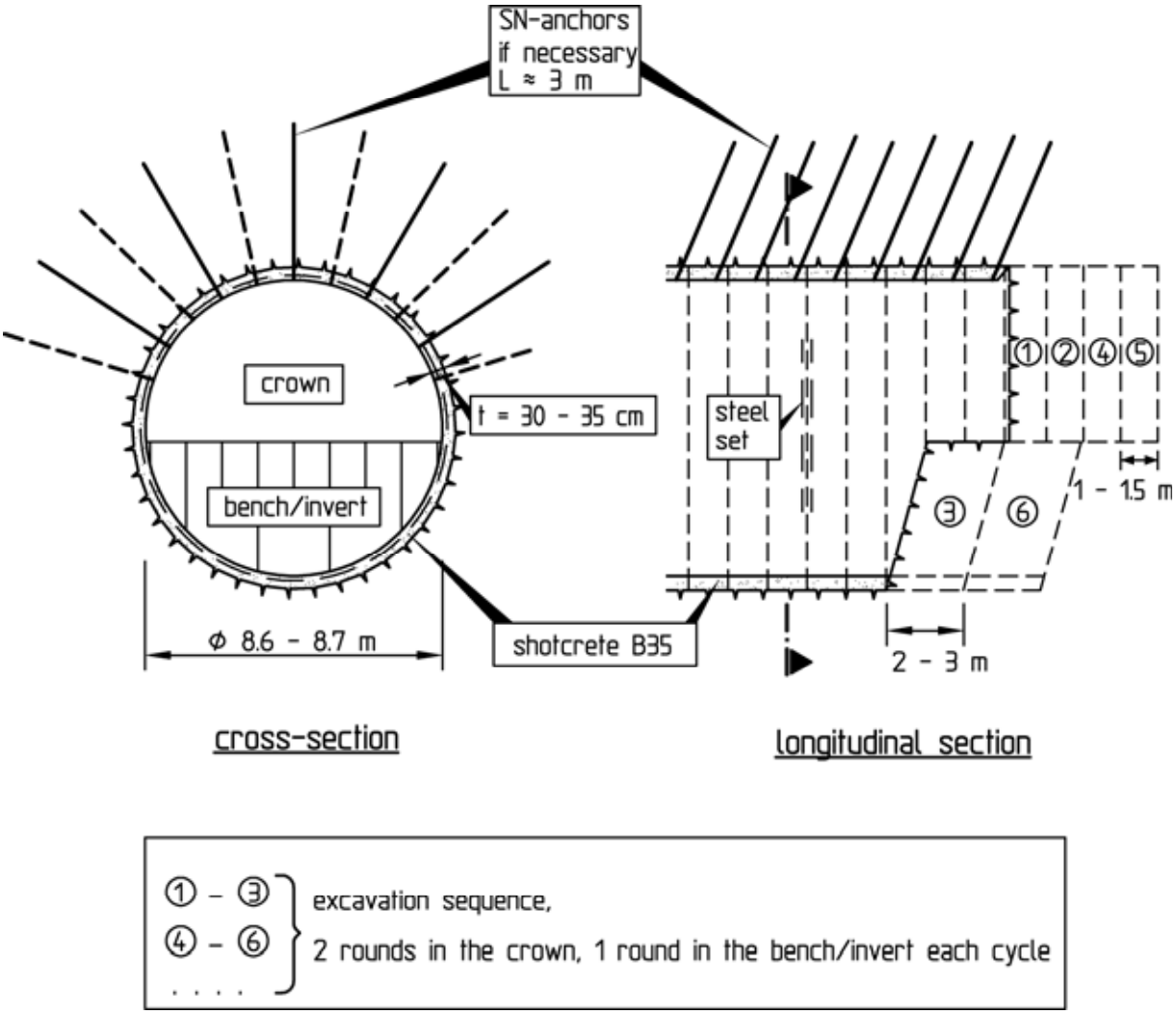

Fig. 6.10: Standard heading in the mudstone, excavation and support

The tunnel cross-section was excavated using tunnel excavators, which were additionally equipped with a heavy hydraulic chisel. Thicker banks of lime-sandstone were loosened by blasting. The round lengths ranged between 1 and 1.5 m in the crown and between 2 and 3 m in the bench/invert (Fig. 6.10). The support was closed at the invert after 4 to 6 m.

In addition to the reinforced shotcrete support of the excavation profile, a systematic anchoring with 3 m long SN-anchors was carried out locally. Steel sets were placed at a spacing of 1 m (Fig. 6.10). The advancing support using spiles, included in the design for more unfavorable rock mass sections, could be completely dispensed with.

In the deep tunnel section, in which the tunnel is located completely within the low-permeability layers consisting predominantly of mudstone, no further measures apart from the low-permeability shotcrete membrane were taken to maintain the groundwater table. In the northern tunnel section, in which the ascending tunnel cuts into the strongly water-bearing layers of the alternating sequence, an advance sealing of water-bearing discontinuities was required to prevent a strong inflow of water through the tunnel face. To this end cement grouting was carried out through boreholes drilled from the tunnel face with an average length of 15 m (Fig. 6.11). Cement based suspensions with water cement ratios of 0.7 to 2 were used for the grouting.

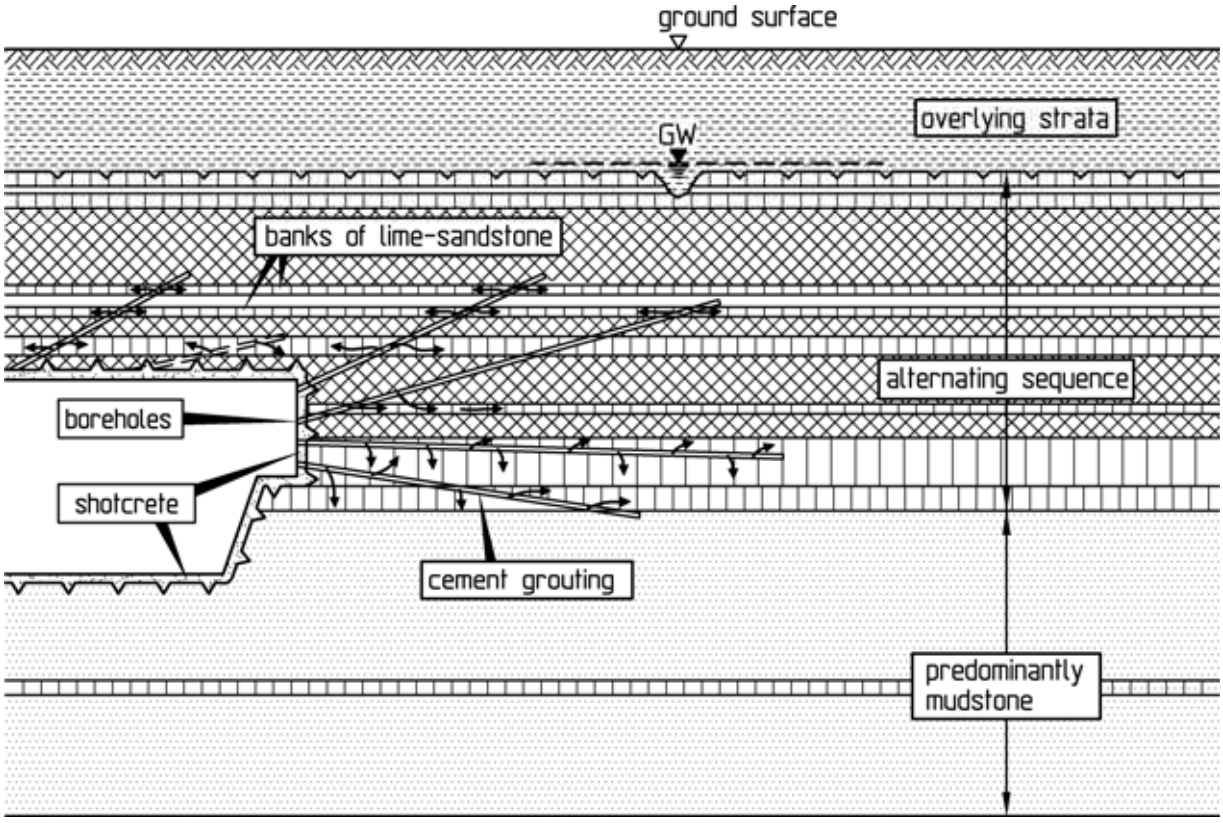

Fig. 6.11: Sealing by advance cement grouting of the alternating sequence

The advance grouting was carried out in sections in three working steps:

1. Sealing of the temporary tunnel face with shotcrete.

2. Construction of a grouting umbrella above the tunnel roof.

3. Construction of a transverse bulkhead in the area of the alternating sequence to seal off the area to be excavated against groundwater flow in longitudinal tunnel direction.

The grouting boreholes were sealed against the borehole head with fabric packers (geotextiles) filled with cement based suspension. During the grouting works the heading had to be interrupted for approx. 2 weeks each time.

By the advance sealing of the alternating sequence stronger inflow of water through the open tunnel face could be prevented to a large extent. Only when the grouting boreholes were drilled (Fig. 6.12), some inflow rates occurred for a short time due to the construction process (Tegelkamp et al., 2000).

Fig. 6.12: Drilling of grouting boreholes

6.1.6 Stability analyses for the design of the shotcrete support

For the dimensioning of the shotcrete support, two- and three-dimensional FE-analyses were carried out using the program system FEST03 (Wittke, 2000). These analyses were based on the characteristic parameters given in Table 6.1. In the Lias α increased horizontal in-situ stresses were taken into account. For the layers consisting predominantly of mudstone $\Delta\sigma_H$ = 1.5 MN/m^2 was specified. The alternating sequence was assigned a value of $\Delta\sigma_H$ = 0.5 MN/m^2. Further analyses were carried out with no additional horizontal stresses assumed, as well as with horizontal stresses in the mudstone increased to $\Delta\sigma_H$ = 2 MN/m^2. In Fig. 6.13, the location of the analysis cross-sections investigated in the design analyses is given in the geological longitudinal section.

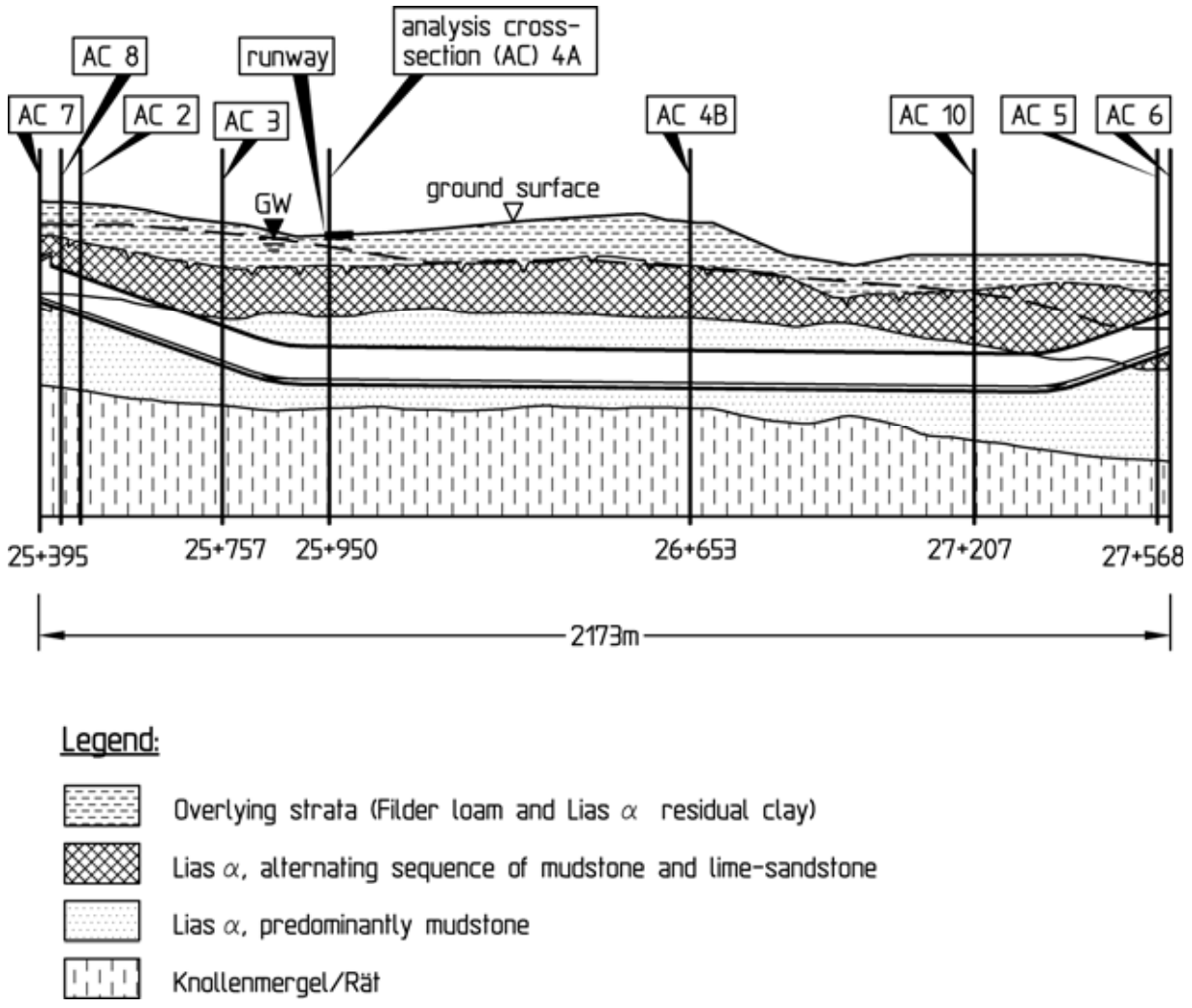

Fig. 6.13: Location of the analysis cross-sections

Fig. 6.14 shows exemplarily the computation section, the FE-mesh, the boundary conditions and the ground profile of a three-dimensional analysis for the area of the airport runway (analysis cross-section 4A, see Fig. 6.13) with an overburden of 21 m.

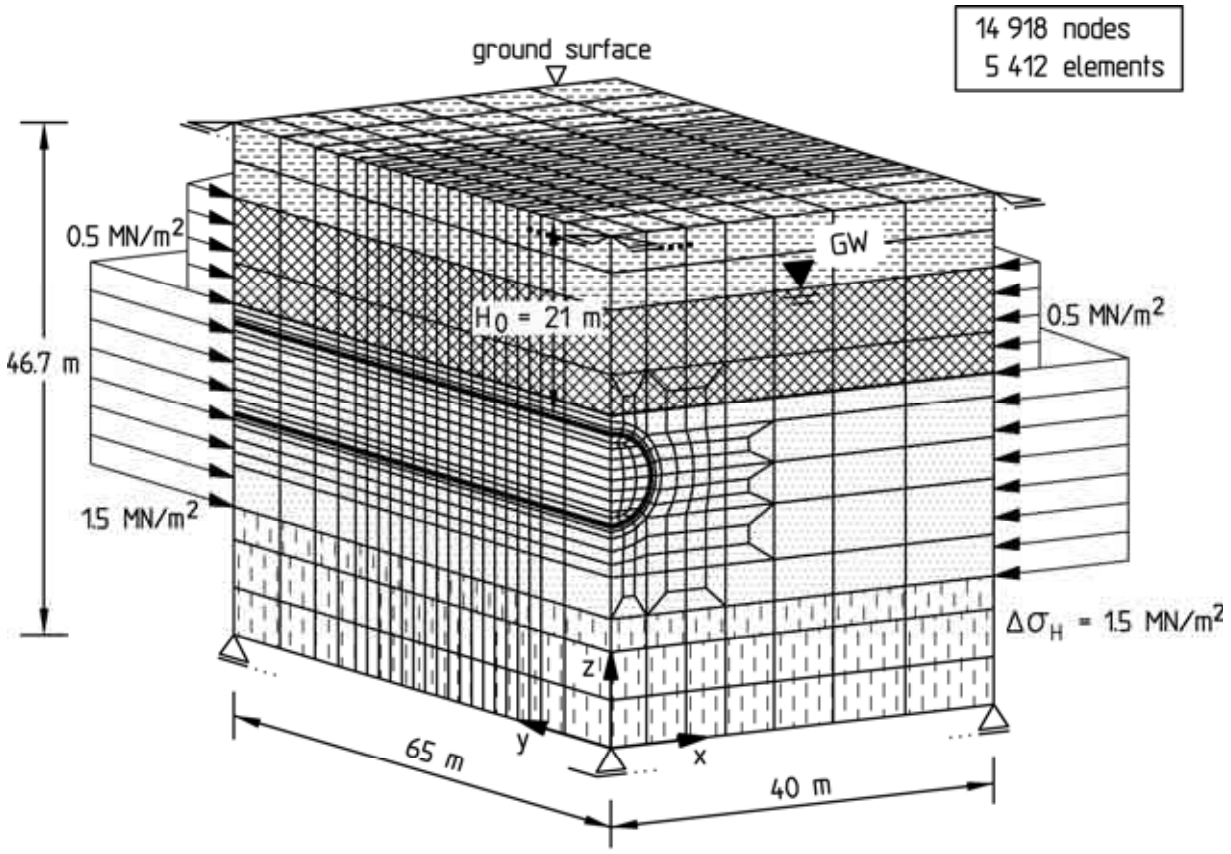

Legend:

- Filder loam and Lias α residual clay
- Lias α, alternating sequence of mudstone and lime-sandstone
- Lias α, predominantly mudstone
- Knollenmergel/Rät

Fig. 6.14: Analysis cross-section 4A, FE-mesh, boundary conditions and ground profile for three-dimensional analyses

In Fig. 6.15 the computation steps chosen for the simulation of the tunnel heading by the "step-by-step" method (Wittke, 2000) are illustrated.

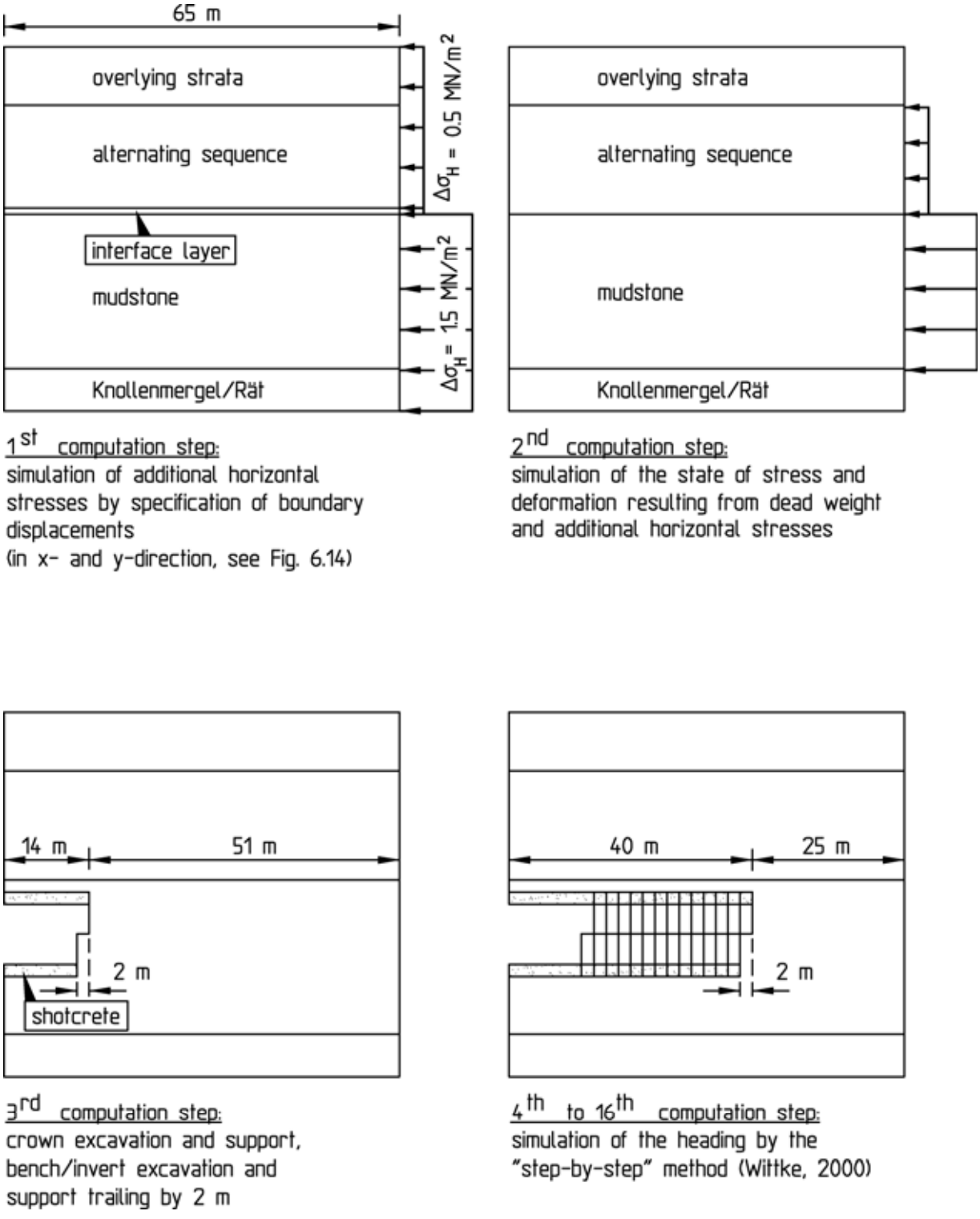

Fig. 6.15: Analysis cross-section 4A, computation steps

In the first two computation steps the in-situ state of stress is determined, taking into account the dead weight of the rock mass and the increased horizontal stresses in the Lias α. To simulate the different horizontal stresses $\Delta\sigma_H$ in the alternating sequence and in the mudstone, the nodes lying on the boundary planes

x = 40 m and y = 65 m (see Fig. 6.14) were assigned horizontal displacements in x- and y-direction corresponding to the respective horizontal stresses $\Delta\sigma_H$. To prevent shear stresses from being transferred across the boundary between the alternating sequence and the mudstone due to the different horizontal displacements, an interface layer is arranged between the two layers. In the 1st computation step, the dead weight is only taken into account for the alternating sequence and the mudstone. The overlying strata, the Rät and the Knollenmergel are assumed to be weightless. In the 2nd computation step the latter two layers are replaced by materials with the same mechanical parameters, however with their dead weight. Since the new materials are installed stress-free in the already deformed corresponding elements (Wittke, 2000) and the horizontal displacements remain unchanged in the 2nd computation step, only the stresses due to dead weight but not the increased horizontal stress $\Delta\sigma_H$ are effective in these layers.

In the 3rd computation step, the excavation and shotcrete support of the crown and the bench and invert, trailing by 2 m, are simulated. Computation steps 4 to 16 include the simulation of the heading according to the "step-by-step" method. In each computation step, the crown and the trailing bench and invert are both advanced by 2 m (Fig. 6.15).

Fig. 6.16 and 6.17 show the stress resultants in the shotcrete membrane determined in this analysis. The representation of the maximum stress resultants along the tunnel in Fig. 6.16 illustrates that the loading of the shotcrete membrane continuously develops with increasing distance from the tunnel face, until the maximum values are reached at a distance of approx. twice the tunnel's diameter. This cross-section is designated the dimensioning section, because the stress resultants determined here have to be considered decisive for the design of the shotcrete membrane (see Chapter 5.3).

The stress resultants M, N and S in the dimensioning section are shown in Fig. 6.17. As expected, great compressive normal thrust exist. Because of the high horizontal stresses the maximum values result in the roof and invert areas. The bending moments are relatively small due to the favorable geometry of the cross-section (circle), and the shear forces follow corresponding to the moment distribution.

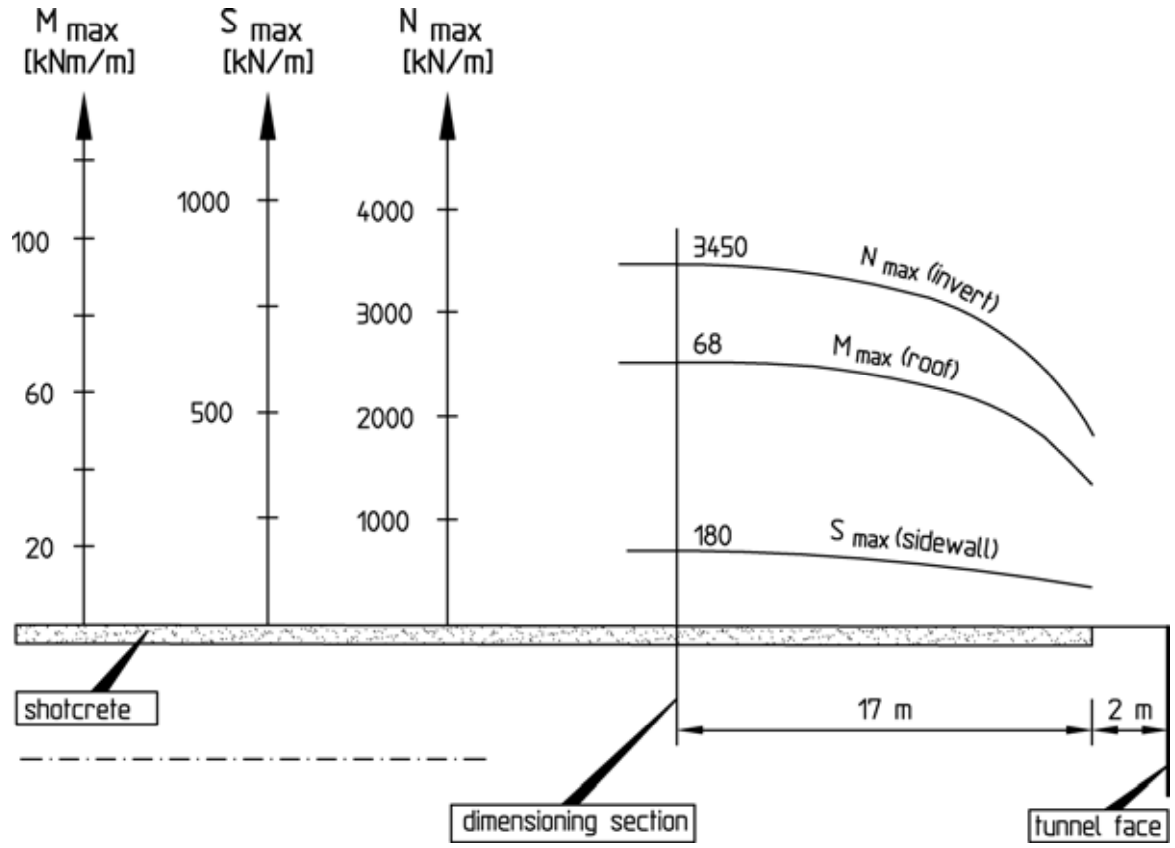

Fig. 6.16: Analysis cross-section 4A, stress resultants vs. distance from the tunnel face, 16th computation step

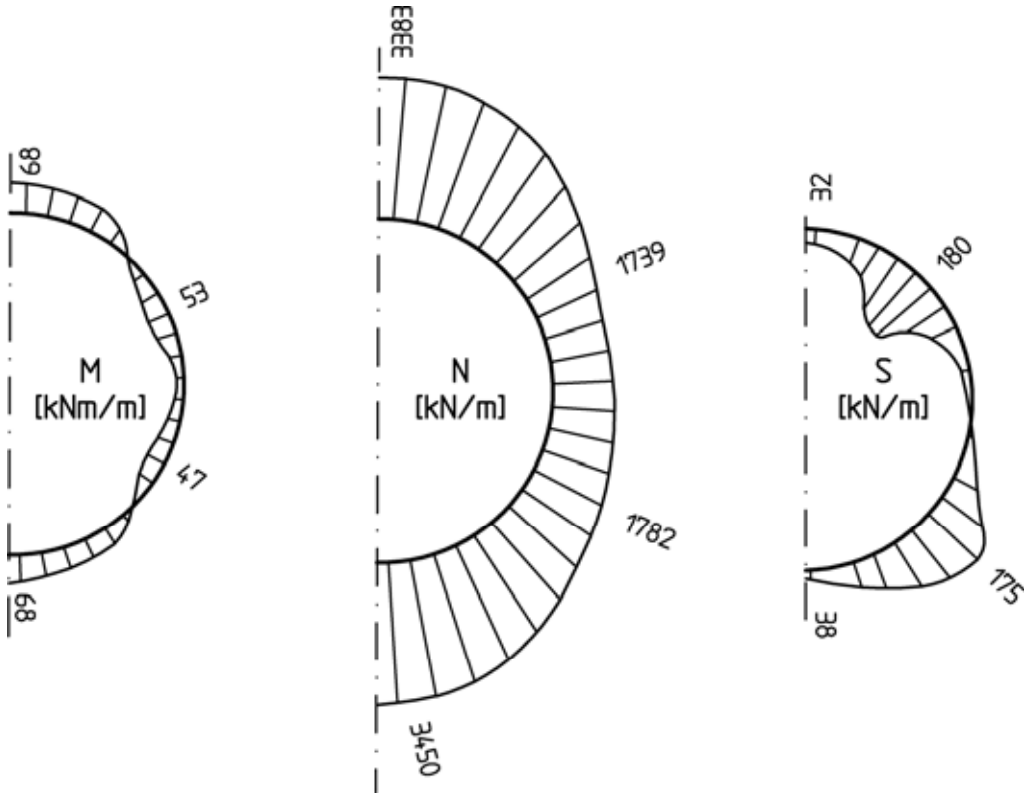

Fig. 6.17: Analysis cross-section 4A, stress resultants in the shotcrete membrane, dimensioning section, 16th computation step

In addition to the three-dimensional analyses, two-dimensional analyses ones were carried out to investigate the influence of a variation of the parameters and of the horizontal in-situ stresses in the Lias α on the loading of the shotcrete membrane.

To model the influence of the displacements occurring in the tunnel face area before the shotcrete membrane is installed, either the computed stress resultants in the shotcrete membrane were reduced in the two-dimensional analyses, or a preceding stress relief was simulated (Wittke, 2000). For the section in which the tunnel's cross-section is located entirely within the alternating sequence, a calibration of the results of two-dimensional analyses on the basis of the results of a corresponding three-dimensional analysis resulted in a stress relief factor according to (4.1) (see Chapter 4.1) of $a_v = 0.35$.

The load case water pressure acting on the shotcrete membrane was investigated in separate two-dimensional FE-analyses. Because the water pressure builds up only at a certain distance from the tunnel face, it suffices to superpose the stress resultants ensueing from the rock mass pressure and the water pressure and to design the shotcrete membrane on the basis of the stress resultants thus obtained.

According to the results of the stability analyses, the shotcrete membrane of the standard tunnel sections could be designed with a thickness of 35 cm for a factor of safety of 1.7 without requiring more than the minimum reinforcement (inside and outside steel fabric mats Q285). The specified limits for the tunneling-induced subsidence and differential subsidence were not exceeded either.

6.1.7 Monitoring

The construction was accompanied by an extensive monitoring program aimed at compliance with all requirements as well as control and optimization of the heading works. This program was coordinated in mutual agreement with the FSG.

The monitoring program included the monitoring of the groundwater level as well as displacement measurements at the ground surface and in the tunnel. Further, stress measurements were carried out in the shotcrete membrane. For the monitoring of the groundwater level, the system of observation wells already existing on the

airport from previous construction and supplemented during the exploration works for the urban railway tunnel could be used.

Fig. 6.18 shows the location of the measuring cross-sections and observation wells as well as the heading location in November 1999. From mid-February to mid-March 2000 the airport runway was undercrossed by the excavation south coming from the northern starting shaft. The excavation north emanating from the southern starting shaft cut through to the excavation south on April 22, 2000 (Fig. 6.18). The tunnel section excavated between November 1999 and April 2000 is specifically marked in Fig. 6.18. The cut-through from lot 601 to the already existing lot 92, which have been constructed before by the cut-and-cover method, was carried out on June 5, 2000.

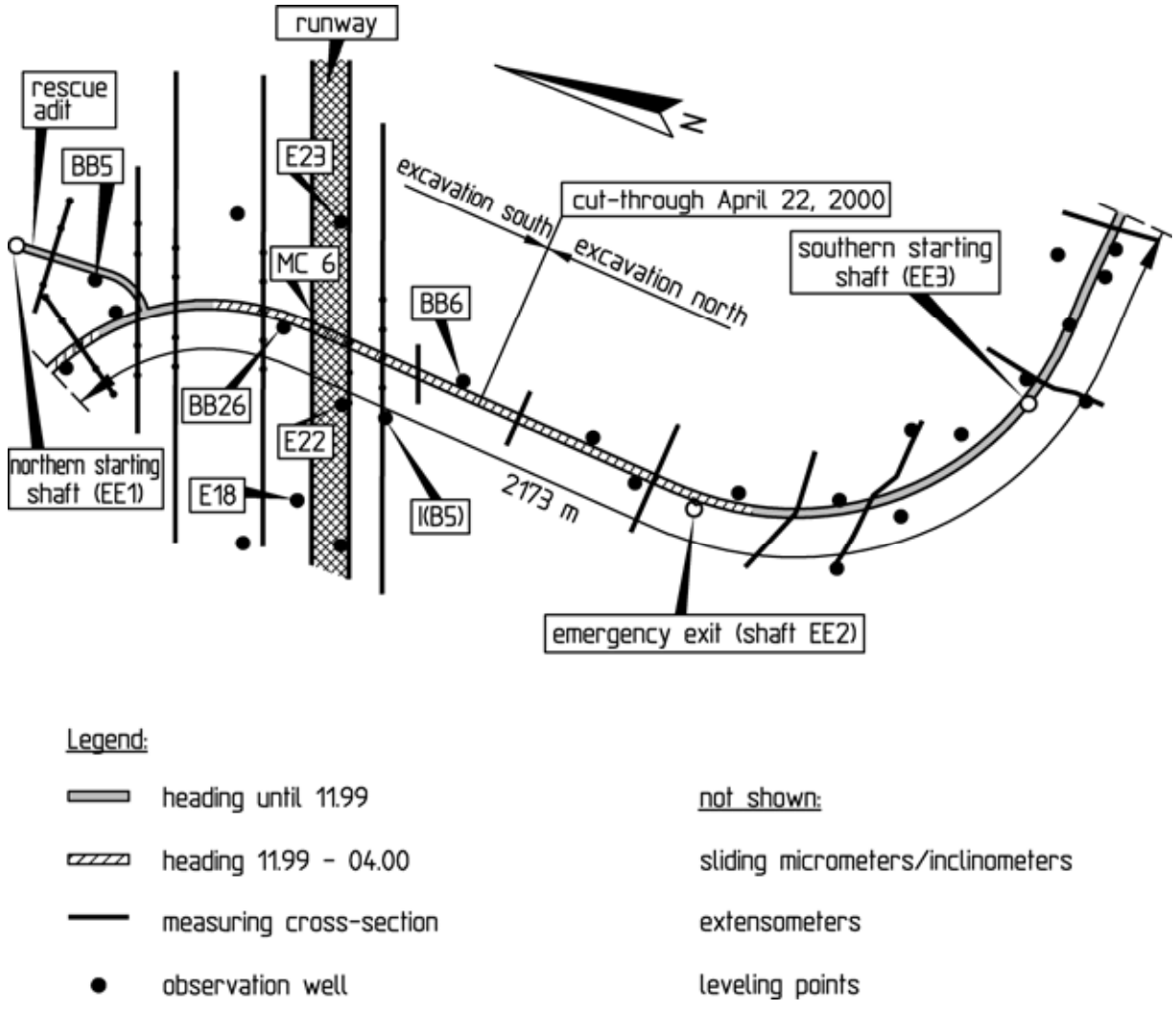

Fig. 6.18: Stuttgart urban railway (lot 601), monitoring program

In Fig. 6.19 the hydrographs of the observation wells in the area of the airport runway are shown for the time between November 1999 and June 2000. For the winter months a general rise of the groundwater level is apparent at all observation wells, which declines again in the spring of 2000. A reaction of the groundwater level to the tunnel heading cannot be recognized. The measured variations in water level can be attributed to the natural course of the groundwater flow and are not related to the tunneling.

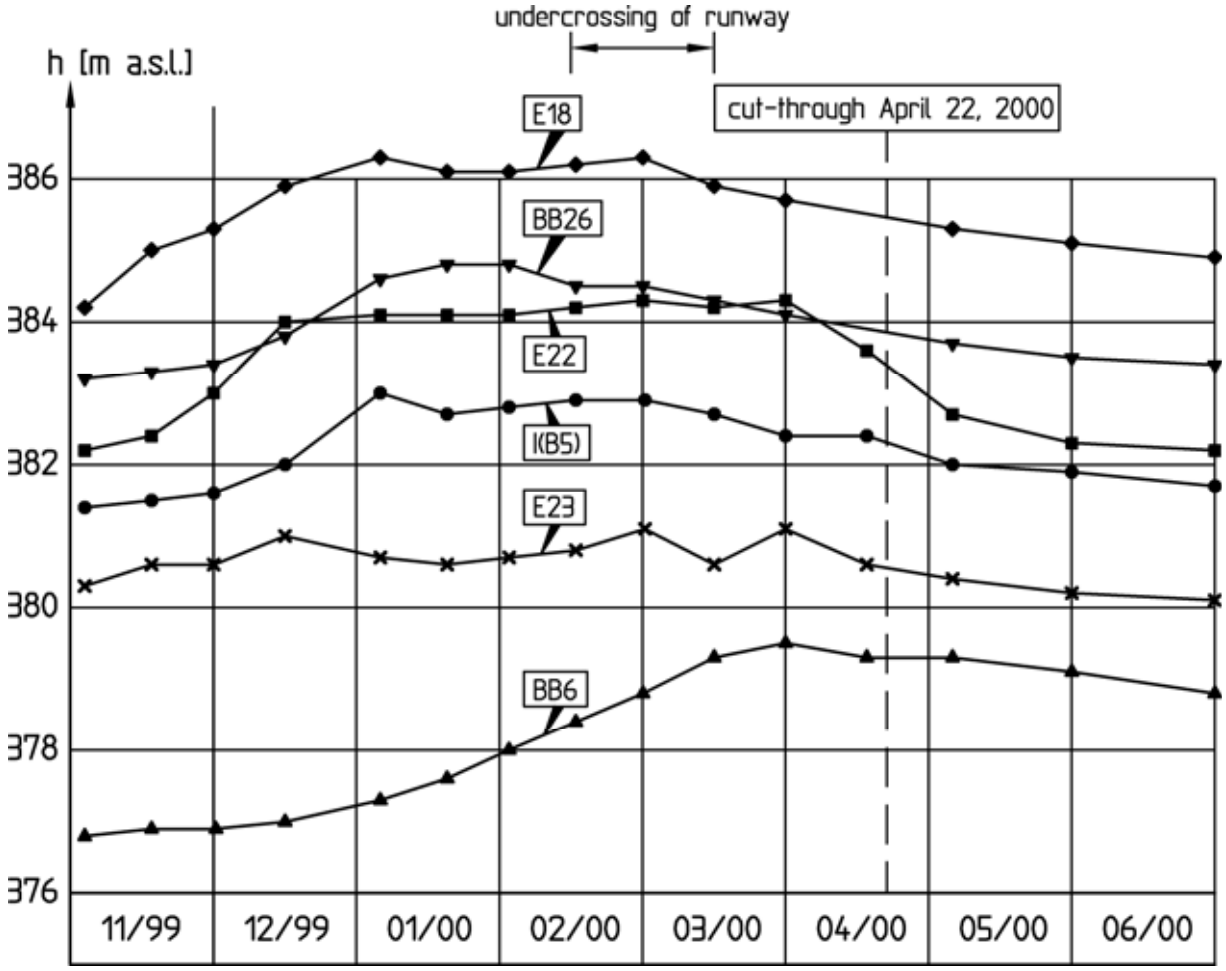

Fig. 6.19: Observation well hydrographs during the undercrossing of the runway of Stuttgart airport

A temporary drop of the groundwater table by a maximum of 2 to 3 m however occurred in the boreholes located in the area of the northern apron beside the rescue adit (Fig. 6.18). This decrease correlates in time with the grouting works carried out in the tunnel section located within the alternating sequence (see Fig. 6.11). With distances of up to 100 m to the observation wells and in view of the limited discharge in the tunnel through the grout-

ing boreholes of approx. 1 l/s, these observations demonstrate the sensitivity of the aquifer in the alternating sequence.

Overall it must be stated, however, that with the advance grouting a large-scale, long-term groundwater lowering could be avoided. Even in the northern apron area, subsidence due to interference with the groundwater did not occur.

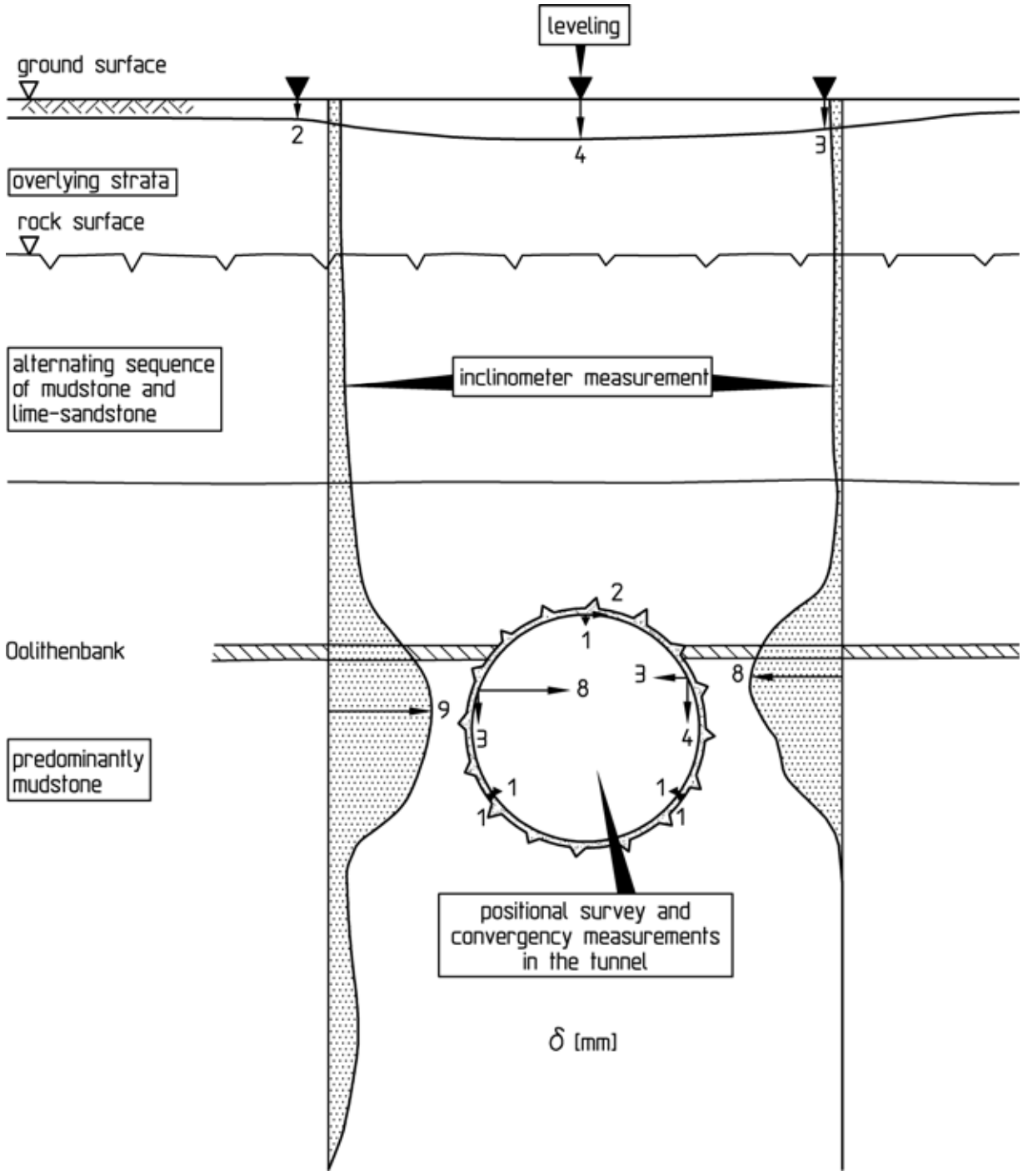

Fig. 6.20: Results of the displacement measurements in MC 6

In Fig. 6.20, the results of the displacement measurements are illustrated exemplarily for measuring cross-section MC 6 (see Fig. 6.18). Here, a tunneling-induced subsidence of 4 mm at the most was measured at the ground surface above the tunnel roof. Along the entire tunnel, predominantly a subsidence of between 4 and 7 mm was determined above the tunnel axis. Because of these comparatively low values, which were markedly smaller than the admissible subsidence of 15 mm, the airport facilities as well as the buildings of Bernhausen, neighboring to the south, could be undercrossed without damage.

Comparatively large horizontal displacements in the ground of up to 9 mm were measured at the level of the tunnel (see Fig. 6.20). This displacement distribution is typical for this construction project and has to be attributed to the increased horizontal in-situ stresses in the Lias α.

6.1.8 Interpretation of the monitoring results

During the construction the displacements measured in the tunnel as well as the tangential stresses measured in the shotcrete membrane were compared to the values computed in the design analyses, which are based on the characteristic parameters (see Table 6.1). The resulting differences can be attributed to the conservative assumptions made in the design analyses, mainly on the high horizontal stresses $\Delta\sigma_H$ assumed in the Lias α (see Fig. 6.14).

To be able to back-analyze the measured results, parameter studies were carried out. The following parameters, which have a large influence on the loading of the shotcrete membrane, were varied:

- Horizontal stresses in the mudstone ($\Delta\sigma_H$),
- deformability of the mudstone layers (E_1, E_2),
- shear strength on the bedding parallel discontinuities in the mudstone (φ_B),
- deformability of the shotcrete membrane (E_{SC}).

The best agreement with the monitoring results was achieved in a comparative analysis, in which a Young's modulus of the shotcrete support of E_{SC} = 2000 MN/m^2 was selected as opposed to the

Young's modulus taken as a basis for the design analyses (E_{SC} = 15000 MN/m^2), and in which the horizontal stress in the mudstone was reduced from 1.5 MN/m^2 (design analysis) to 1.0 MN/m^2 (Table 6.2).

	Design analyses	**Comparative analysis**
Shotcrete	E_{SC} = 15000 MN/m^2	E_{SC} = 2000 MN/m^2
Mudstone with single layers of lime-sandstone	$\Delta\sigma_H$ = 1.5 MN/m^2	$\Delta\sigma_H$ = 1.0 MN/m^2

Table 6.2: Comparison analysis for the interpretation of monitoring results: Differences to the construction design analyses

The low modulus of E_{SC} = 2000 MN/m^2 accounts for the deformability development as well as the creep properties of the shotcrete. Because of the short round lengths and the early closing of the support ring, the shotcrete is loaded in the present case at a very young age, in which it still possesses a low strength and a high deformability as well as a high creep potential (see Chapter 2.1). The value of E_{SC} = 15000 MN/m^2 used in the design analyses therefore represents a conservative assumption, by which the loading of the shotcrete membrane is overestimated.

A good agreement with the measured values can however only be achieved if the water pressure and the seepage forces are accounted for that act on the ground and the shotcrete membrane during construction.

Since the water permeability of the alternating sequence is high compared to the one of the mudstone, there is no significant decrease of piezometric heads within the alternating sequence. Almost the entire decrease of piezometric heads thus occurs in the mudstone. Fig. 6.21 shows qualitatively the flow net with its equipotential lines and streamlines which represents the groundwater flow towards the tunnel. Thus, as an approximation, the entire water pressure p_w resulting from the difference in elevation between the groundwater table and the top boundary of the mudstone layer acts on the mudstone layer. The loading of the shotcrete membrane due to the groundwater flow towards the tunnel can there-

fore be replaced as an approximation by a surface load p_w acting on the mudstone layer (Fig. 6.21).

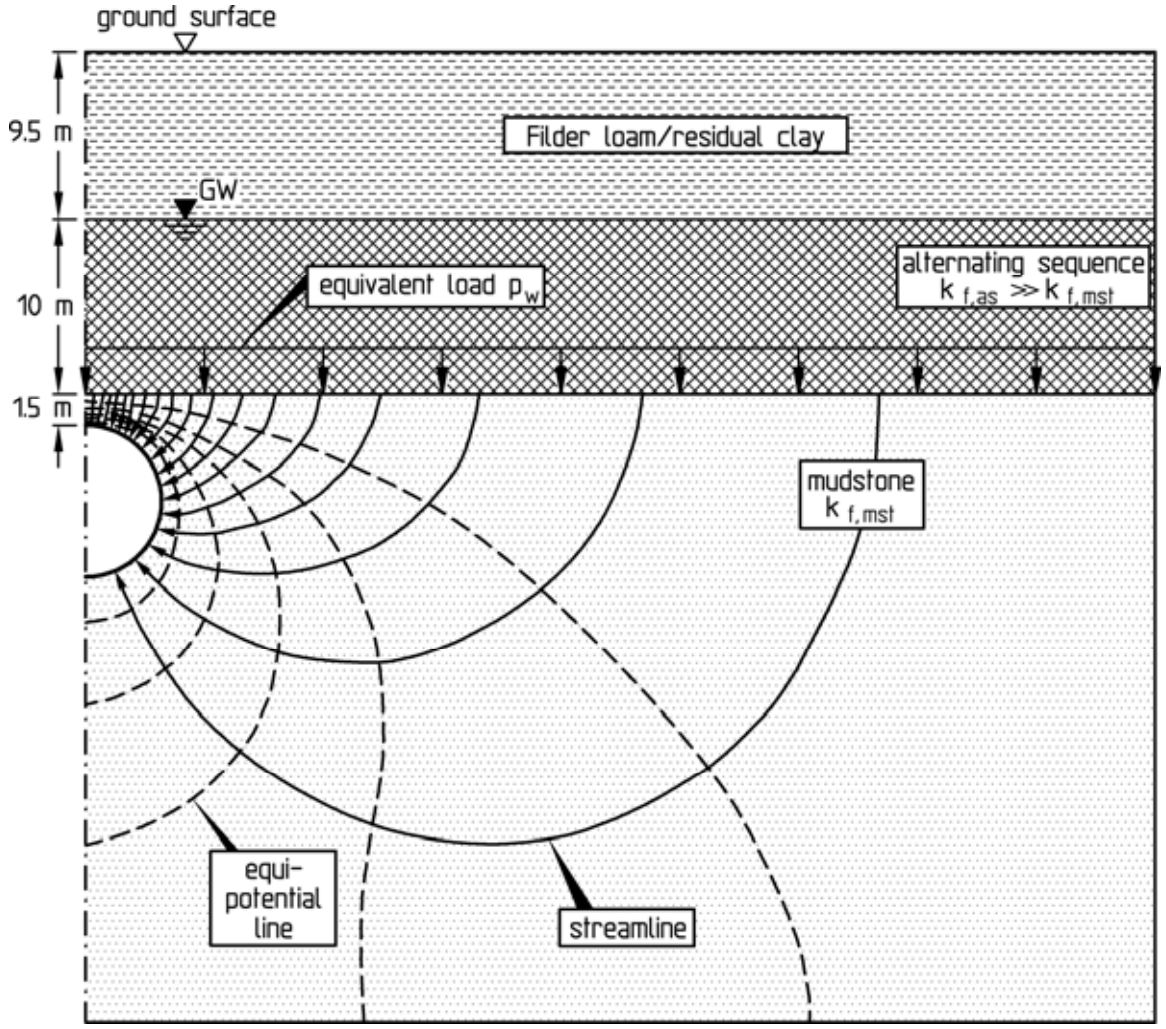

Fig. 6.21: Qualitative distribution of equipotential lines and streamlines in the mudstone and replacement of the water pressure by an equivalent load

Fig. 6.22 illustrates the determination of the stresses and deformations resulting from the flow towards the tunnel in two computation steps. In the 1st computation step the surcharge from the water pressure p_w is applied onto the mudstone layer. In the 2nd computation step, the excavation and the installation of the shotcrete membrane are simulated. The rock mass and the shotcrete are assumed weightless here. The deformations and the loading of the shotcrete membrane can therefore be determined approximately by superposing the deformations and stresses computed for the load cases "rock mass pressure" and "water pressure on the mudstone layer".

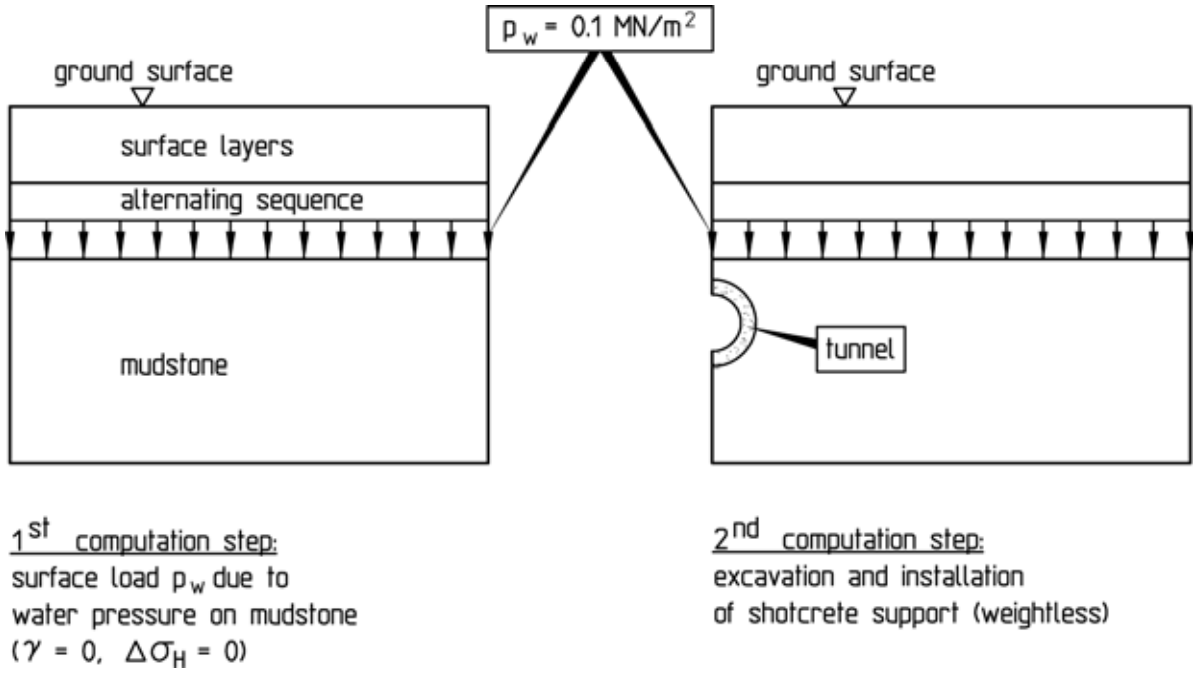

Fig. 6.22: Computation steps to determine the stresses and deformations resulting from the flow towards the tunnel

Fig. 6.23 shows the comparison between the measured and the computed values of the displacements of the tunnel contour and the tangential stresses in the shotcrete.

The comparison between measured and computed displacements is based on so-called "representative displacements" determined as the mean values of the displacements measured in different cross-sections. It can be seen that the representative displacements can be captured by the analyses if the water pressure is taken into account (Fig. 6.23).

Around the circumference of the shotcrete membrane differing tangential stresses were measured. The very low stresses measured in the roof area (see Fig. 6.23, bottom left), are not considered representative. In the other areas the measured tangential stresses are captured by the analysis.

During the heading of the rescue adit as well, geotechnical monitoring was carried out (see Fig. 6.18). The representative displacements of the tunnel contour and the tangential stresses in the shotcrete measured in the rescue adit are pictured in Fig. 6.24 (left). The displacements are somewhat smaller than the representative displacements in the urban railway tunnel. The meas-

ured tangential stresses are markedly higher in the roof than the tangential stresses shown for in the shotcrete membrane of the urban railway tunnel.

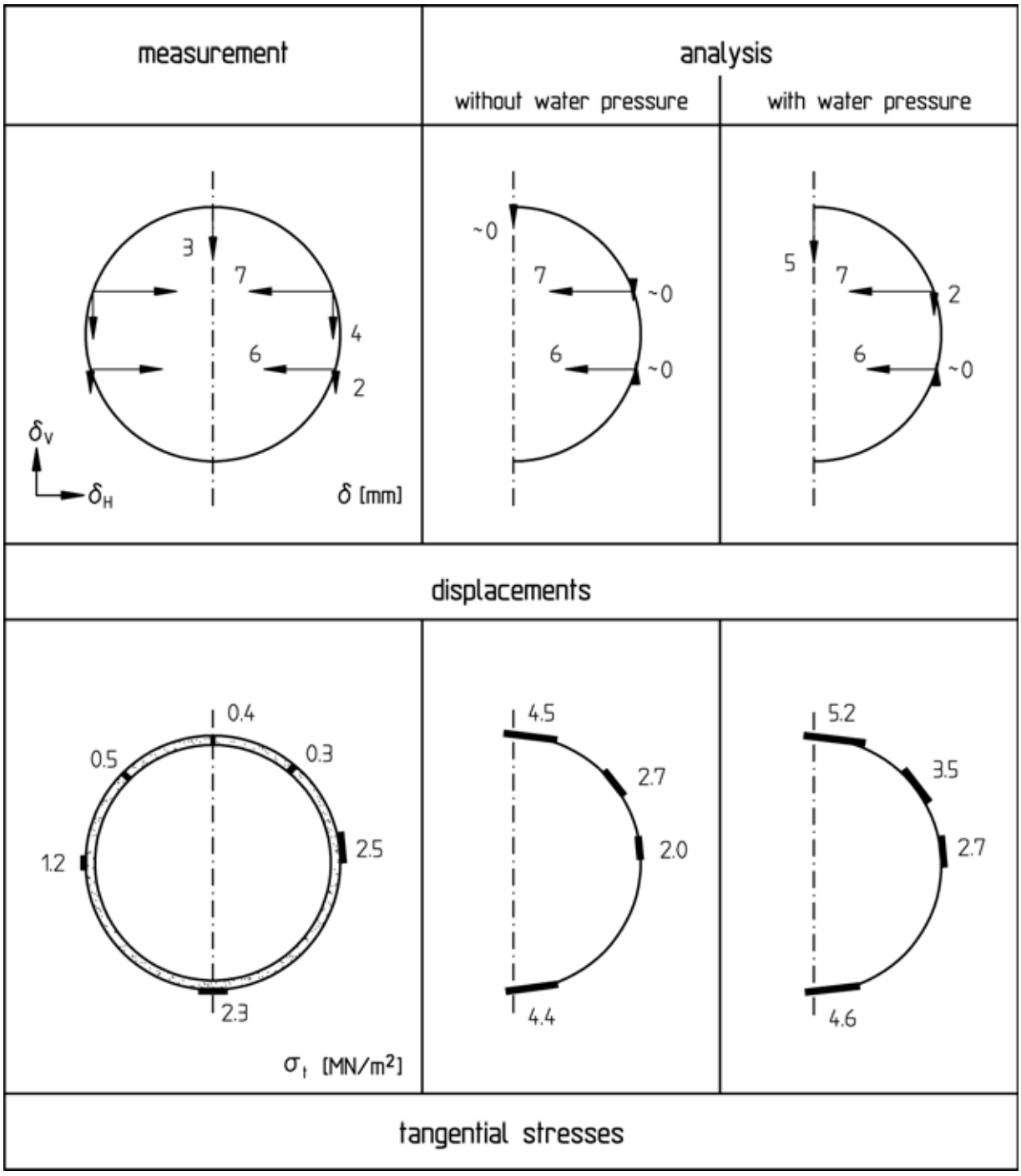

Fig. 6.23: Comparison of the measured displacements and tangential stresses in the runway area with the corresponding values computed with and without consideration of the water pressure

The monitoring results obtained in the rescue adit can be back-analyzed with the same parameters as the monitoring results in the urban railway tunnel. In Fig. 6.24 the monitoring results are compared with the values computed with and without consideration of the water pressure. If the water pressure is taken into account, the displacements as well as the tangential stresses agree well.

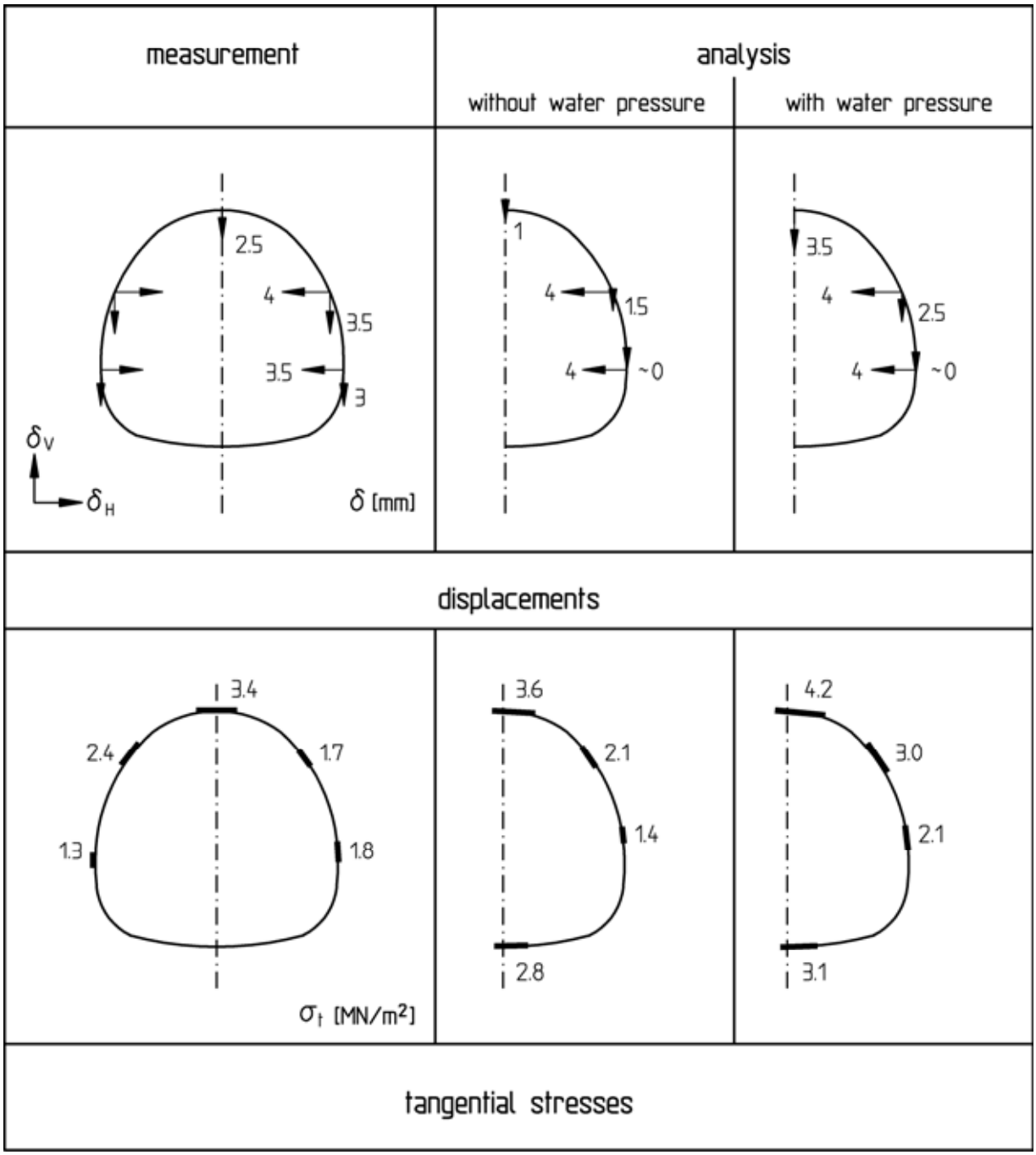

Fig. 6.24: Comparison of the measured displacements and tangential stresses in the rescue adit with the corresponding values computed with and without consideration of the water pressure

6.1.9 Conclusions

Stuttgart airport was to be undercrossed by a tunnel with low to medium overburden. The water table is located above the tunnel roof, and settlement-sensitive layers are locally encountered at the ground surface. Because of the demands with respect to the admissible subsidence, groundwater lowering had to be avoided during tunneling. Accordingly, the shotcrete membrane had to be dimensioned for the water pressure. It had to be further taken into account for the design of the shotcrete membrane that the Lias α, in which the tunnel cross-section is located, shows increased horizontal in-situ stresses and low strengths on the bedding parallel discontinuities.

This task was solved by the following measures:

- Full-face excavation with a stepped tunnel face and an early closing of the support ring,

- construction of a low-permeability shotcrete membrane with high strength,

- specification of a circular profile which is statically favorable for the design of the shotcrete membrane,

- sealing of water-bearing discontinuities in the alternating sequence of mudstone and lime-sandstone by advance grouting.

By these measures, the tunnel could be excavated with very small subsidence of the ground surface. There was no interference with air traffic at any time.

It further showed that the transient seepage flow analyses and two- and three-dimensional stability analyses carried out in the course of this project with the program systems HYDOPO and FEST03 (Wittke, 2000) represented an essential contribution towards the design, the statics and the specification of the excavation and support measures.

6.2 Freeway tunnel "Berg Bock" near Suhl, Germany

6.2.1 Introduction

In the course of the new freeway (Autobahn) A71 connecting Erfurt and Schweinfurt (Kleffner, 2000), the "Berg Bock" freeway tunnel was excavated between the exit Suhl/North and the intersection Suhl (Fig. 6.25). The two tubes each 2700 m in length from north to south pass through the Suhl granite, the base sediments and porphyrite as well as, after passing the southern edge fault, the layers of the Lower Triassic sandstone (Fig. 6.26).

Fig. 6.25: Tunnel Berg Bock, site plan

The two tunnel tubes were driven mainly by the full-face excavation method within a construction time of approx. 10 month. With four tunnel faces, maximum performances of approx. 30 m/d were attained.

6.2.2 Structure

Two tunnel tubes, eastern tube and western tube each 2700 m in length were constructed (Fig. 6.27). The spacing of axis of both tubes ranges between approx. 23 m at the northern portal and approx. 30 m at the southern portal. Each tube comprises two traffic lanes each 3.75 m wide and two emergency sidewalks (Fig. 6.28). The excavated cross-section of the tunnel ranges between 80 m^2 and 100 m^2 (Fig. 6.28 and 6.29). The alignment dips continuously towards the southern portal with 1.1 %. The maximum overburden amounts to approx. 190 m (Fig. 6.26).

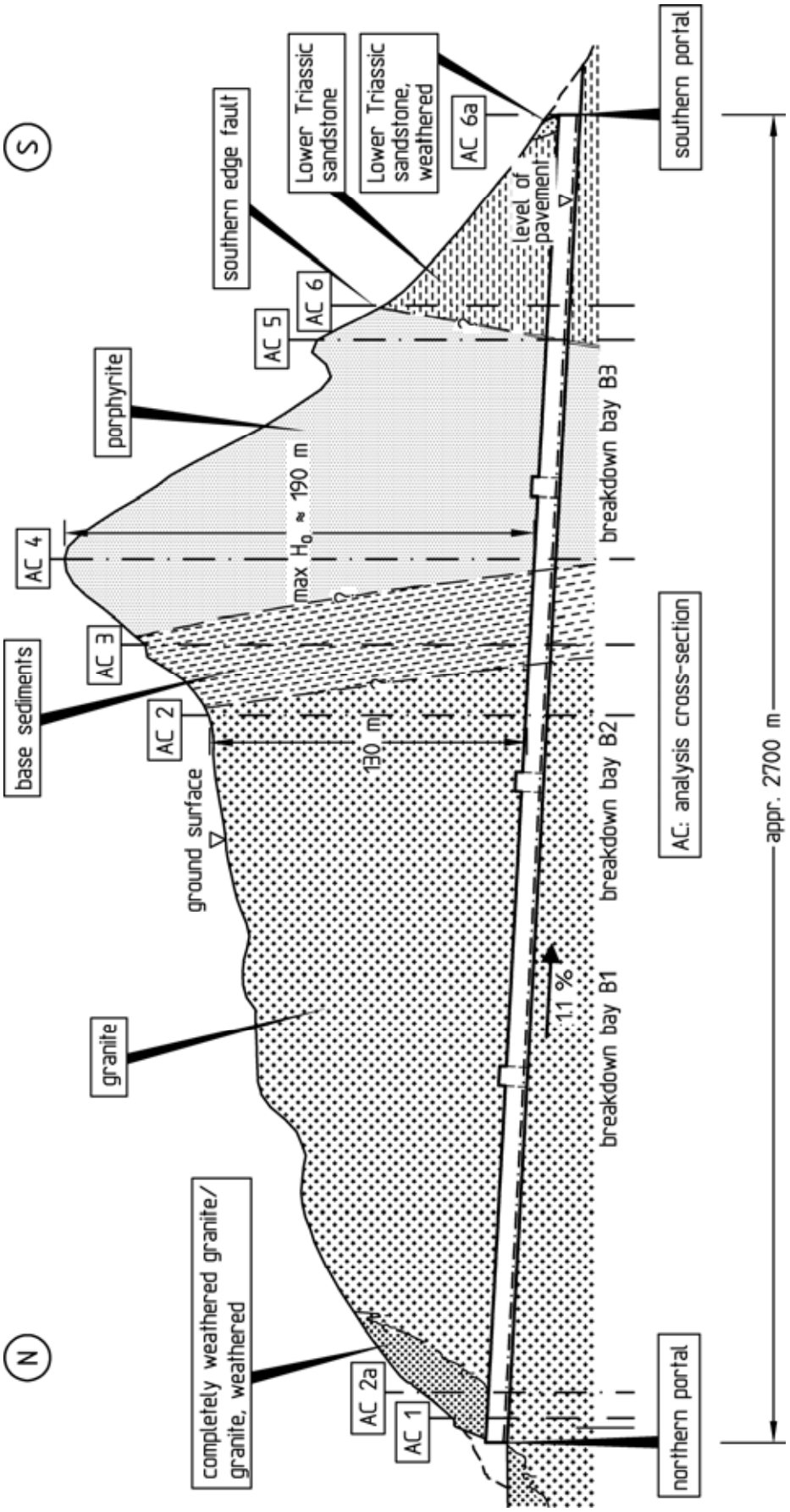

Fig. 6.26: Tunnel Berg Bock, geological longitudinal section with analysis cross-sections

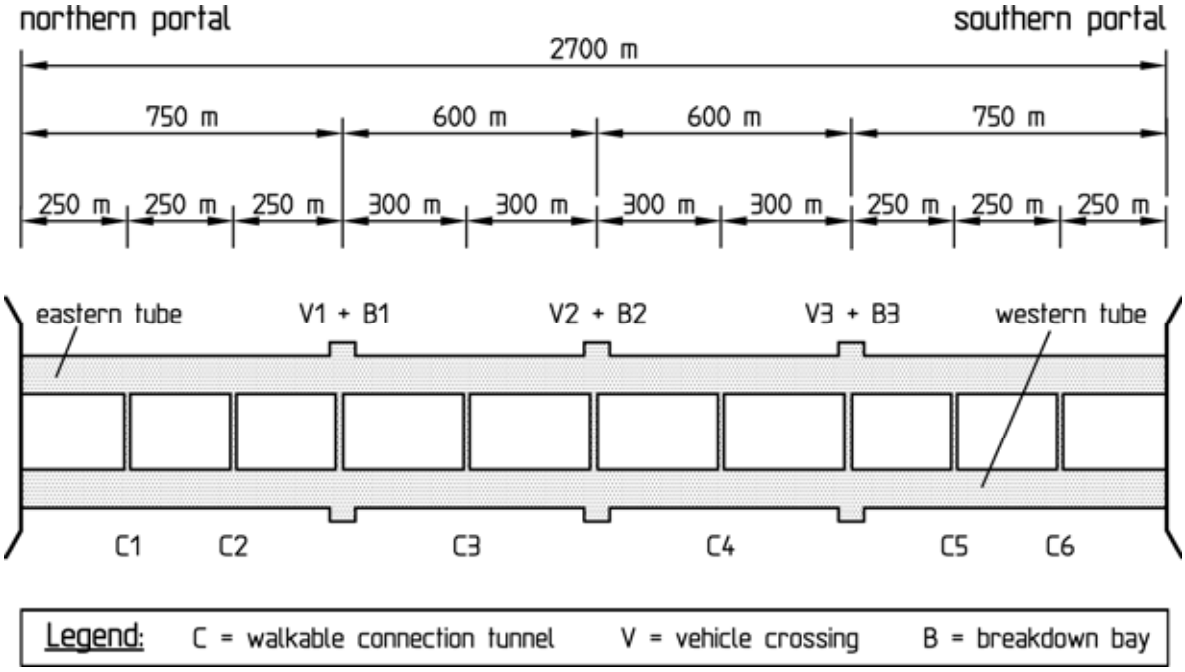

Fig. 6.27: Safety conception

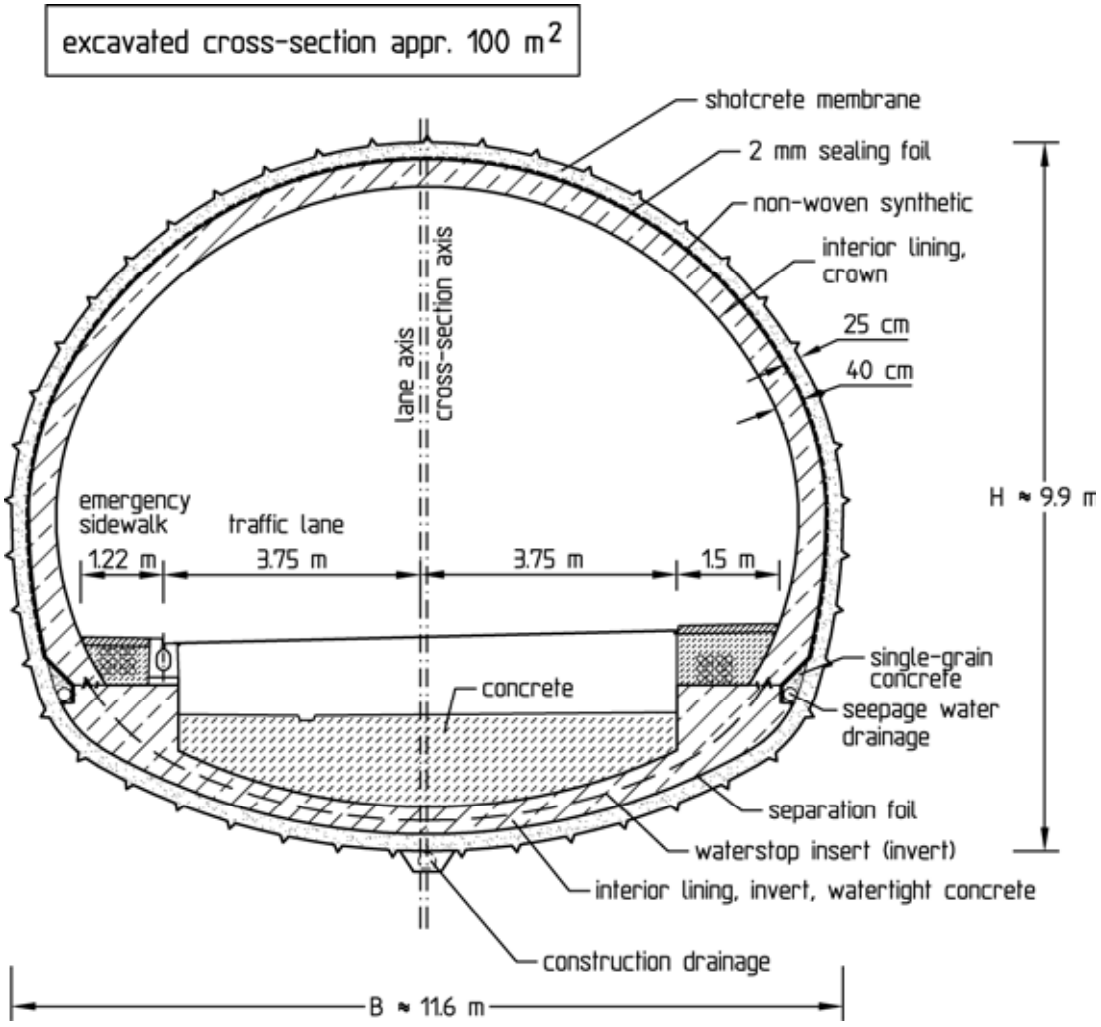

Fig. 6.28: Tunnel cross-section with closed invert in weathered rock mass, portal zones

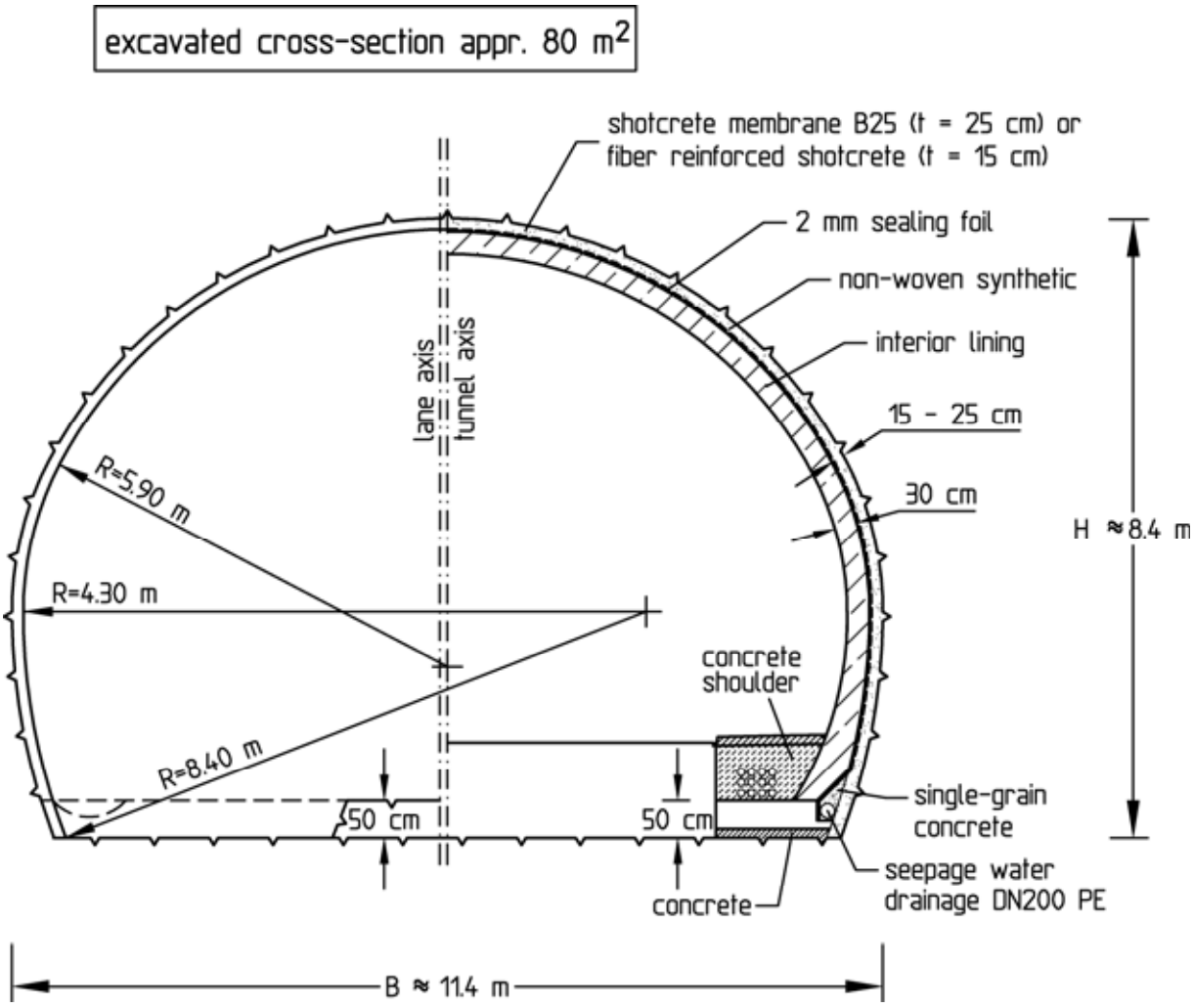

Fig. 6.29: Tunnel cross-section with open invert in stable rock mass

The safety conception is based on the German standard for the equipment and the operation of road tunnels (RABT, 1994). This standard was currently revised on the basis of the evaluation of several fire accidents in tunnels happened in recent years. Thus, additional, supplementary demands on the safety conception had to be fulfilled at short notice in the final planning for the tunnel Berg Bock (Schmidtmann and Erichsen, 2001).

The safety conception comprises nine connection tunnels between the tubes at distances of ≤ 300 m (Fig. 6.27). The connection tunnels are equipped with emergency call niches and fire protection locks. Three breakdown bays are furthermore situated in each tunnel tube with distances of ≤ 600 m. Three connection tunnels located close to the breakdown bays are passable for rescue vehicles. Besides that, emergency call niches and niches provided with

fire extinguishing devices are located in each tube at distances of ≤ 150 m. Fire emergency lights are installed on one side of each tube at distances of 24 m (Table 6.3).

Installation	Distance	Quantity
connection tunnels	≤ 300 m	9
breakdown bays	≤ 600 m	2 x 3
emergency call niches	≤ 150 m	2 x 19
hydrant niches	≤ 150 m	2 x 19
electrical niches	approx. 180 m	2 x 14
niches for drainage flushing shafts on both sides of the lanes	50 - 80 m	2 x 104
road sign displays	approx. 300 m	2 x 9
jet fans	approx. 300 m	2 x 9
fire emergency lighting	24 m	2 x 110

Table 6.3: Installations for operational safety

In the areas of the portals weathered rock of the Lower Triassic sandstone and completely weathered granite, respectively, were encountered (Fig. 6.26). In these sections the tunnel tubes were carried out with an approx. 11.6 m wide and approx. 9.9 m high mouth-shaped cross-section with a closed invert and an excavated cross-section of approx. 100 m². The thickness of the shotcrete membrane (concrete grade B 25 corresponding to C 20/25) is 25 cm. The interior lining (concrete grade B 35 corresponding to C 30/37) is 40 cm thick (Fig. 6.28).

In the remaining sections, located in stable rock mass, a cross-section of approx. 11.4 m width and approx. 8.4 m height with an open invert and an excavated cross-section of approx. 80 m² was carried out. The tunnel walls mainly were supported by fiber reinforced shotcrete with a concrete grade of B 45 corresponding to C 35/45 and a thickness of t = 15 cm. Locally reinforced shotcrete with a concrete grade of B 25 and a thickness of t = 25 cm was installed. The shotcrete membrane was carried out with radii of R = 5.9 m, R = 4.3 m and R = 8.4 m. The 30 cm thick interior lining with a concrete grade of B 35 was founded on 50 cm high concrete shoulders with the same grade (Fig. 6.29).

Between the interior lining and the shotcrete membrane a non-woven synthetic and as a sealing a 2 mm thick foil were installed (Fig.

6.28 and 6.29). In the tunnel sections with closed invert between the interior lining and the shotcrete membrane a separation foil was installed at the invert (Fig. 6.28). Thus, in this area between interior lining and shotcrete membrane no tensile and shear forces can be transferred.

Both tubes were carried out as fully drained road tunnels. The seepage water was drained off by two lateral drainage pipes in the area of the lower sidewalls and the gradient of the tunnel of 1.1 % (Fig. 6.28 and 6.29). Flushing shafts for the washing of the drainage ducts are provided at distances of 50 to 80 m on both sides of the lanes.

Fig. 6.30 shows the northern portal of the Berg Bock tunnel.

Fig. 6.30: Tunnel Berg Bock, northern portal

6.2.3 Ground and groundwater conditions

The ground profile is shown in Fig. 6.26 in a geotechnical longitudinal section. The ground conditions and the overburden height are approximately the same for both tunnel tubes.

In the starting area at the northern portal, the granite is predominantly decomposed. The tunnel cross-section is alternatingly located here in hard, mostly strongly jointed granite and in completely decomposed granite.

In the further course of the tunnel, unweathered, mostly very hard granite was encountered. The rock is streaked with a multitude of veins of different thickness. The rock mass is compact, with a joint spacing of more than 1 m, to narrowly jointed, and in some areas it is traversed by joints with large extent.

Fig. 6.31: View of the working face in the Lower Triassic sandstone

The granite is followed by the base sediments (sand-, mud- and siltstone). In the area of the highest cover, the tunnel is located in the porphyrite, which is predominantly hard to very hard and slightly to narrowly jointed. After that, the tunnel crosses the southern edge fault, which consists of water-bearing, strongly decomposed and mylonized zones with a thickness of a few decimeters. In the last tunnel section, the tunnel is located in the Lower Triassic sandstone (Fig. 6.26).

The layers of the Lower Triassic sandstone and the base sediments consist of an alternating sequence of sandstone and mudstone. The widely persistent bedding parallel discontinuities are mostly horizontal in the Lower Triassic sandstone (Fig. 6.31) and predominantly steeply inclined in the base sediments. The joints normal to the bedding usually end at the bedding parallel discontinuties.

The groundwater table is located up to 180 m above the tunnel roof.

6.2.4 Excavation and support

Heading in completely weathered granite

In the area of the northern portal (Fig. 6.26), the following supporting measures were carried out:

- Preceding drainage borings,
- preceding pipe umbrella,
- crown heading with closed invert,
- tunnel face support core.

The round lengths ranged between 0.75 and 1.0 m. A heading performance of approx. 1 m/d was achieved in the area of the completely weathered granite.

Heading in granite and porphyrite

Stable rock mass jointed to varying degrees was encountered in the unweathered granite and porphyrite. The rock mass conditions allowed a full-face blasting excavation of the tunnels in these areas (Fig. 6.32). Mainly excavation class A0 was applied with a round length of up to 3.5 m (Fig. 6.33). In part, an even greater round length was chosen during construction. By the use of steel fiber shotcrete (t = 15 cm) with a fiber content of 40 kg/m^3 for the support of the excavation contour, the expenses for the support were kept low (Fig. 6.33). Anchors were installed as required depending on the jointing.

Fig. 6.32: Loading of blastholes during the full-face excavation in granite

With this optimized heading scheme, approx. 2 to 3 rounds could be achieved per day and tunnel face. The heading performance thus amounted to up to 10 m/d per tunnel face. For the 4 tunnel faces, maximum performances of ≥ 30 m/d were reached.

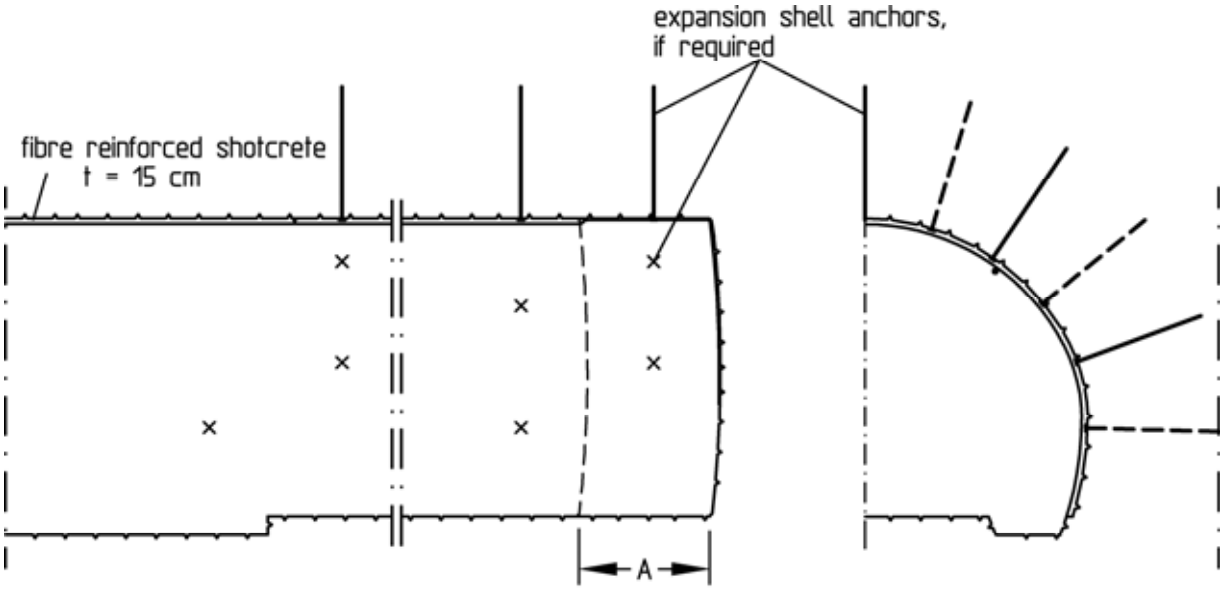

excavation class	A0
excavation method	drill and blast
unsupported round lengths	≤ 3.50 m
shotcrete	B45, t = 15 cm
reinforcement	steel fibers 40 kg/m³
steel sets	GI 100 at the joints of the concrete blocks (spacing: 12m)
anchors	expansion shell anchors, if required, l_A = 3.6 m
tunnel face support	—
advancing support	—
trailing of the shoulders	independent of the full-face excavation

Fig. 6.33: Excavation and support in granite and porphyrite, excavation class A0 (full-face excavation)

Heading in Lower Triassic sandstone and base sediments

In these layers, a crown heading with closed invert and trailing bench excavation was carried out. In order to support the tunnel face and the working area against the dropping of so-called "coffin lids", if the bedding was approximately horizontal, preceding spiles were installed. In areas with the bedding dipping moderately steeply towards the tunnel, a support core was left standing to support the tunnel face.

A performance of approx. 4 to 5 m per day and tunnel face was achieved with this heading technique.

Heading schedule

Both tunnel tubes were excavated within some 10 months each, corresponding to an average heading performance of approx. 9 m per day and tube.

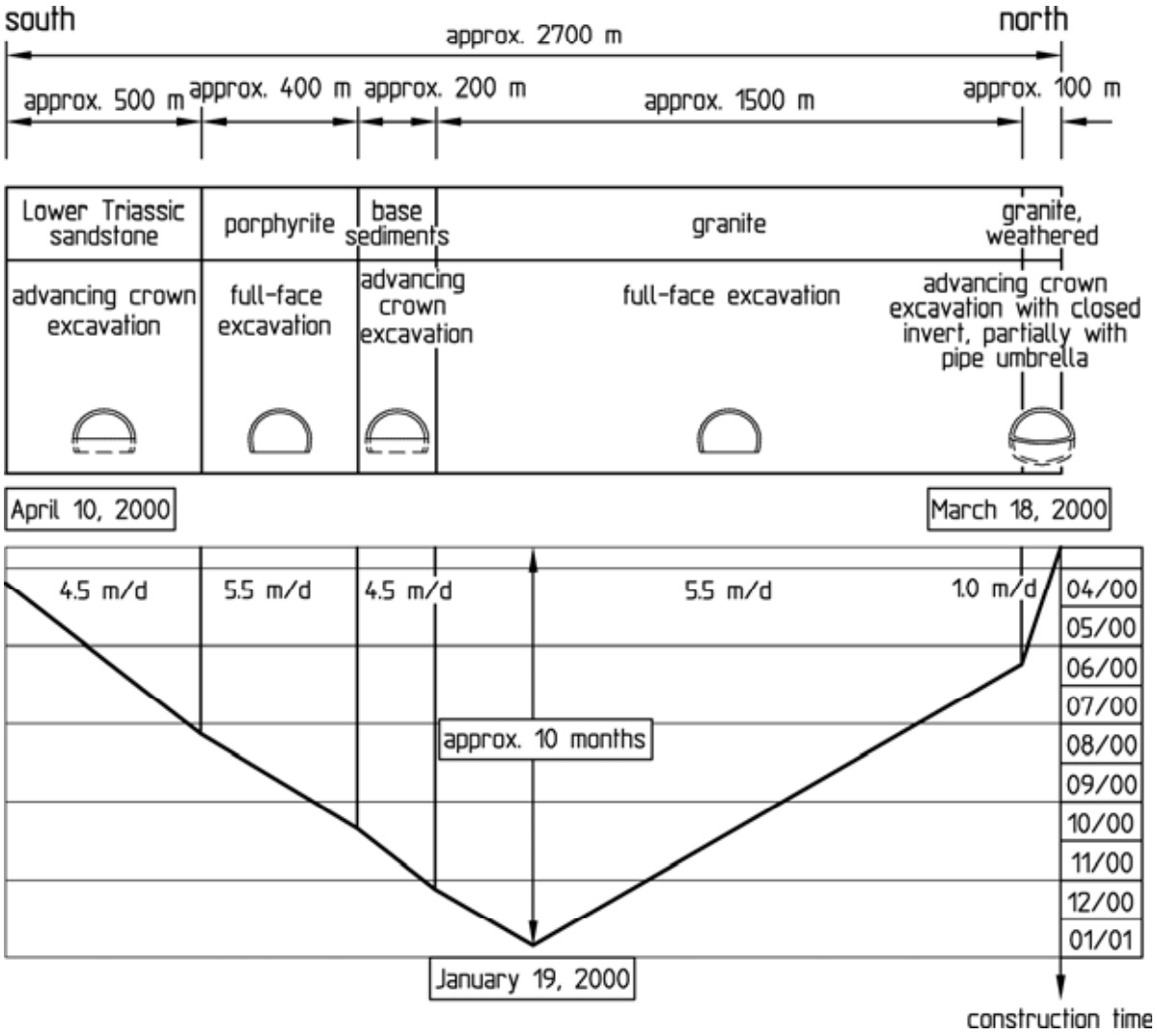

Fig. 6.34: Heading progress of the eastern tube

Fig. 6.34 shows exemplarily the heading progress over time for the eastern tube (see Fig. 6.27). The western tube was excavated in parallel with the eastern tube by so-called opposite heading. The eastern tube was successfully cut through on January 19, 2001. The cut-through of the western tube and thus the heading of the entire tunnel was celebrated on February 2, 2001.

6.2.5 Stability analyses for the stages of construction and design of the shotcrete support

To analyze the stability during construction and to design the shotcrete support, two-dimensional FE-analyses were carried out using the program system FEST03 (Wittke, 2000). A total of eight analysis cross-sections shown in Fig. 6.26 (AC 1 to AC 6, AC 2a and AC 6a) were investigated.

Fig. 6.35 shows exemplarily the FE-mesh, the boundary conditions, the ground profile and the parameters for analysis cross-section AC 2, which was used to analyze the stability of the tunnel tubes in the granite. The overburden amounts to 130 m (see Fig. 6.26).

Due to symmetry, only one tunnel tube is modeled as a simplification. The plane of symmetry lies at the center of the rock pillar between the two tunnel tubes. Such a model is to be considered conservative with respect to the loading of the shotcrete membrane, because this way a simultaneous excavation of both tunnel tubes is simulated.

The specified computation section consists of a 1 m thick slice with a width of 75 m (x-direction). The height amounts to 157 m. The FE-mesh consists of 2135 isoparametric elements with 13004 nodes. As boundary conditions, vertically sliding supports are introduced for the nodes of the vertical boundary planes (x = 0 and x = 75 m). For the nodes of the lower boundary plane (z = 0) horizontally sliding supports are specified (Fig. 6.35). All nodes are assumed fixed in y-direction.

The tunnel cross-section is entirely located in the granite. Below the ground surface, two 11 m thick layers of decomposed granite and slightly weathered granite, respectively, are simulated. The assumed mechanical parameters for these layers are also given in Fig. 6.35. The loading modulus of the unweathered granite was assumed as E_L = 15000 MN/m^2. Underneath the tunnel's invert an un-

loading modulus was specified in the analyses which at 30,000 MN/m^2 was twice as high as the loading modulus (Fig. 6.36).

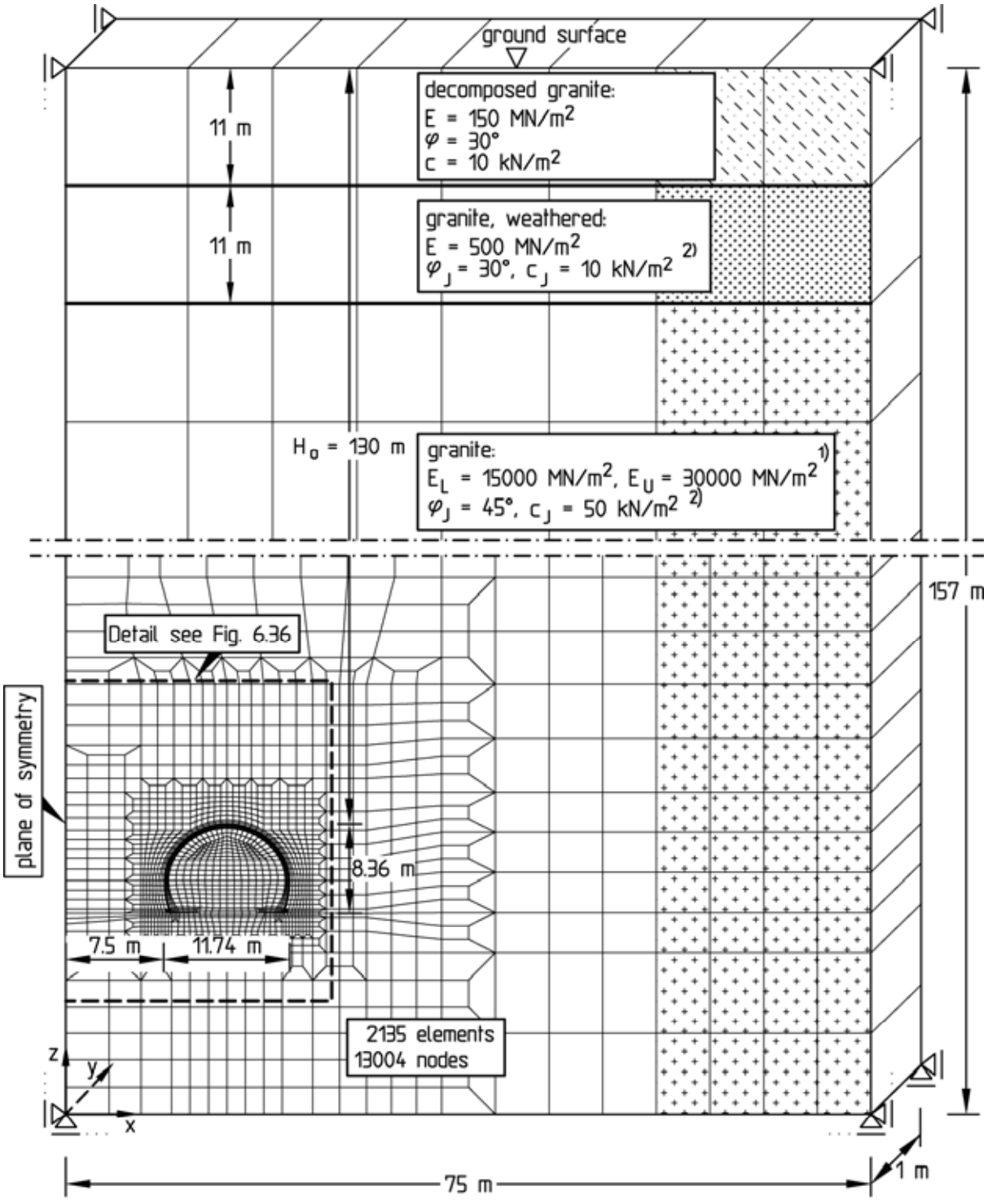

1) E_L : modulus of loading, E_U : modulus of unloading

2) J : joints with randomly distributed orientations (isotropic shear strength)

Fig. 6.35: Analysis cross-section AC 2 (shotcrete support), FE-mesh, boundary conditions, ground profile and parameters

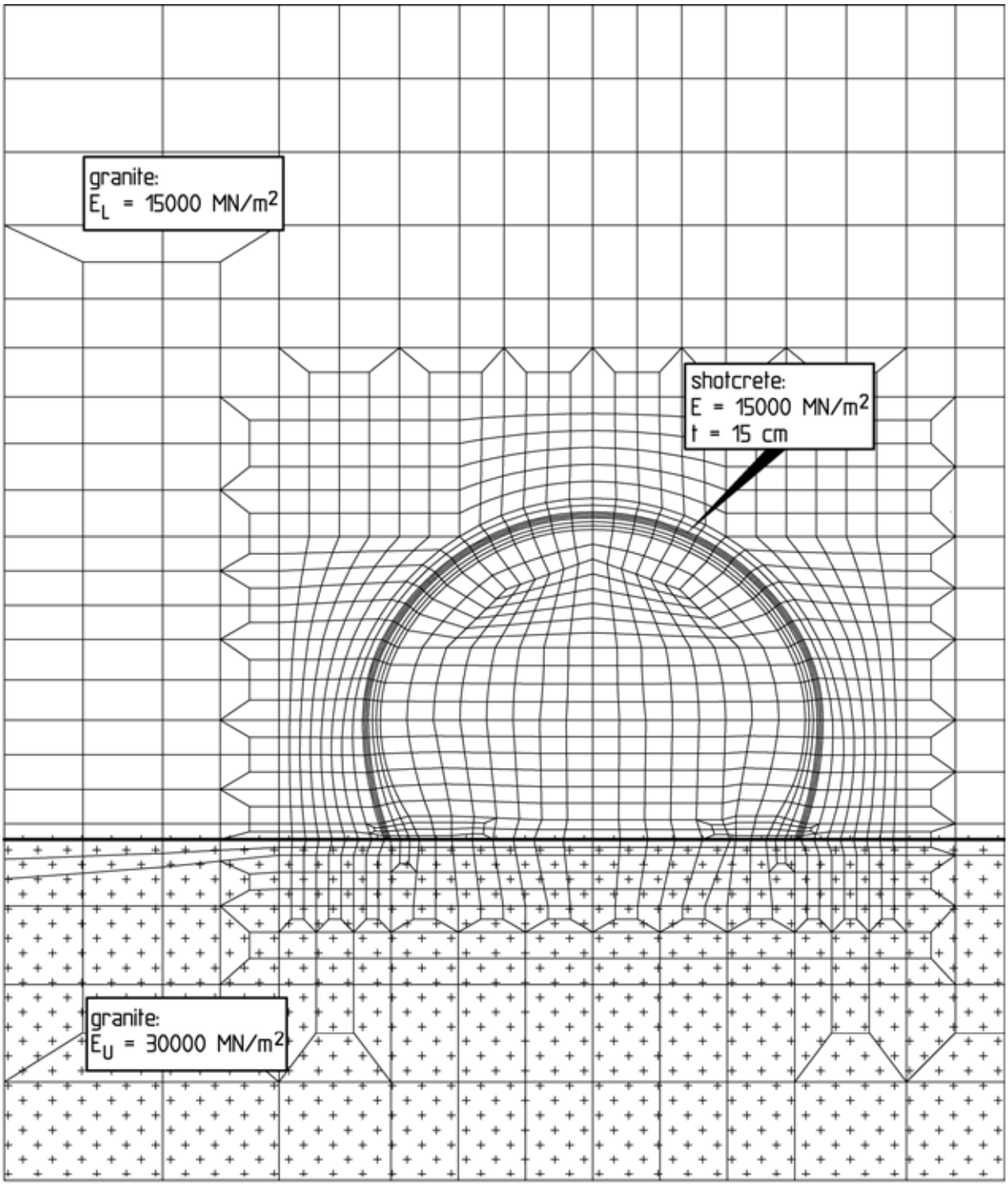

Fig. 6.36: Analysis cross-section AC 2 (shotcrete support), FE-mesh, detail

The orientations of the joints which are present in the granite were not clearly determined. Thus randomly distributed joint orientations were assumed. The rock mass therefore was modeled with

an isotropic strength with shear parameters of φ_J = 45° and c_J = 50 kN/m^2 (Fig. 6.35).

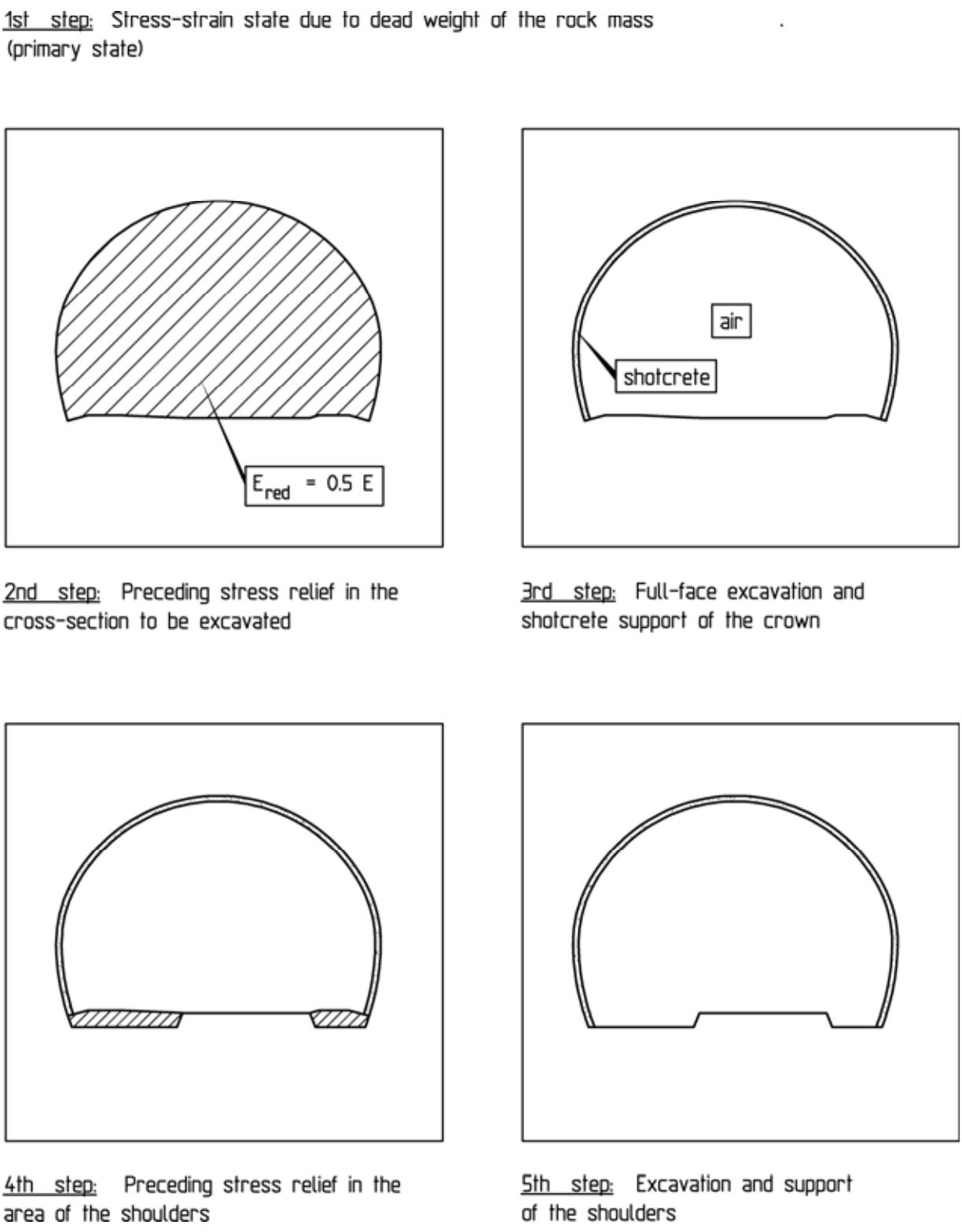

Fig. 6.37: Analysis cross-section AC 2 (shotcrete support), computation steps

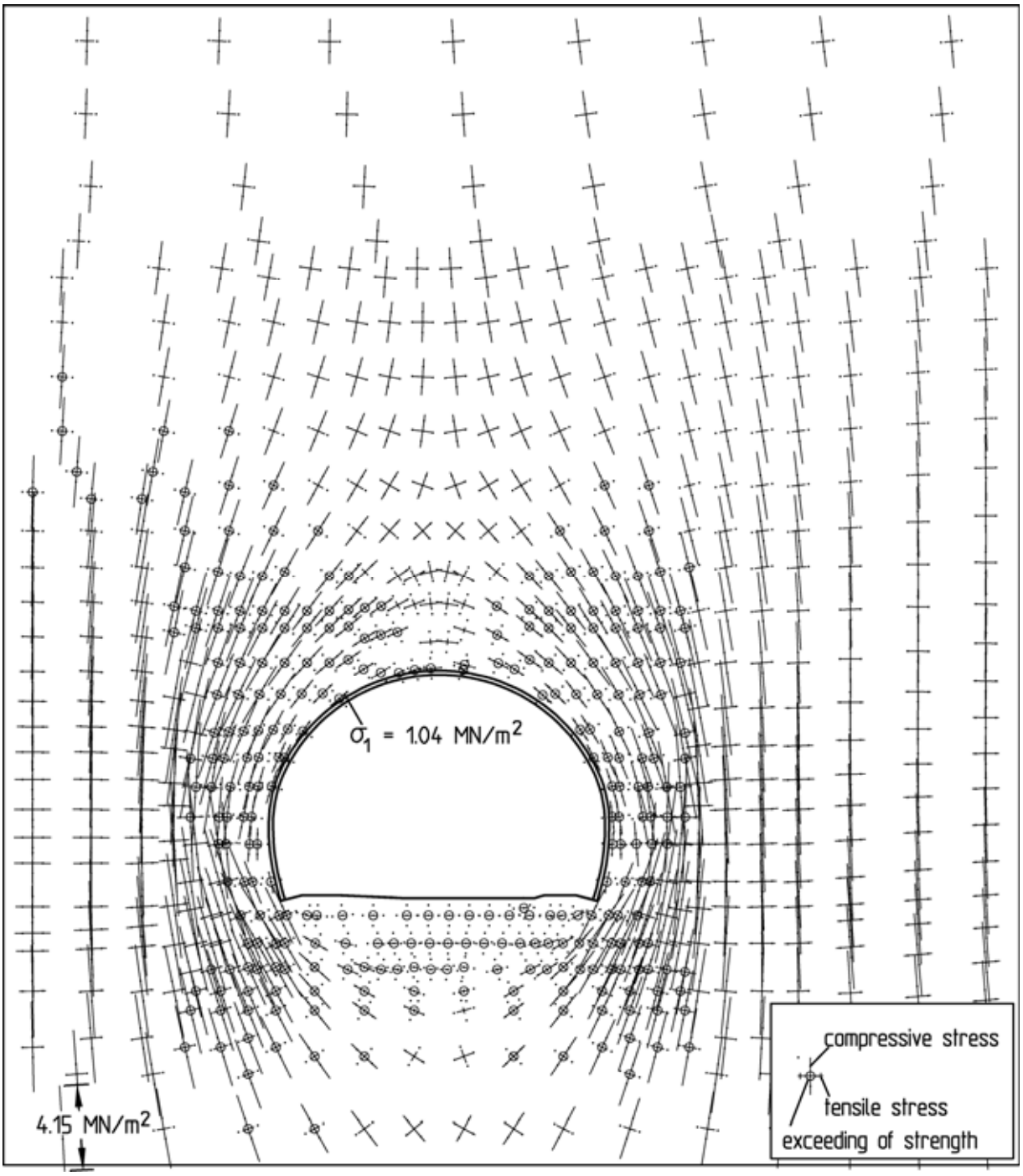

Fig. 6.38: Analysis cross-section AC 2, principal normal stresses and rock mass areas in which strength is exceeded, 3rd computation step

For the shotcrete, a statically effective Young's modulus of 15000 MN/m^2 was assumed taking into account the hardening during the application of the load (Fig. 6.36).

In Fig. 6.37 the computation steps are outlined. In the 1st computation step, the state of stress and deformation resulting from

the dead weight of the ground is determined (primary state). In computation steps 2 and 4, a preceding stress relief is each simulated in those areas of the cross-section, of which the excavation and the shotcrete support are simulated in computation steps 3 and 5, respectively. The stress relief factor according to (4.1) is specified as $a_v = 0.5$.

Fig. 6.38 shows the principal normal stresses in the rock mass around the excavation after the full-face excavation and the installation of the shotcrete support at the end of the 3rd computation step. The stress redistribution that occurred with the excavation as well as the areas of exceeded strength can be recognized. Although these areas extend around the entire circumference of the excavation, a pronounced arching is apparent. Due to the low deformability of the rock mass ($E = 15000$ MN/m^2, see Fig. 6.35), the shotcrete membrane is only marginally loaded by the rock mass and thus takes on a slightly stabilizing and assisting function only.

In Fig. 6.39 the heading-induced displacements computed for the full-face excavation are shown. The total computed roof subsidence amounts to 3.3 mm (3rd – 1st computation step, Fig. 6.39a). In the 2nd computation step (preceding stress relief) the displacements preceding the heading are determined. The shotcrete membrane is therefore only loaded in the 3rd computation step. The displacement of the excavation profile resulting from this loading (3rd – 2nd computation step) is shown in Fig. 6.39b. Thus the computed displacement of the shotcrete membrane amounts to 2.1 mm at the roof.

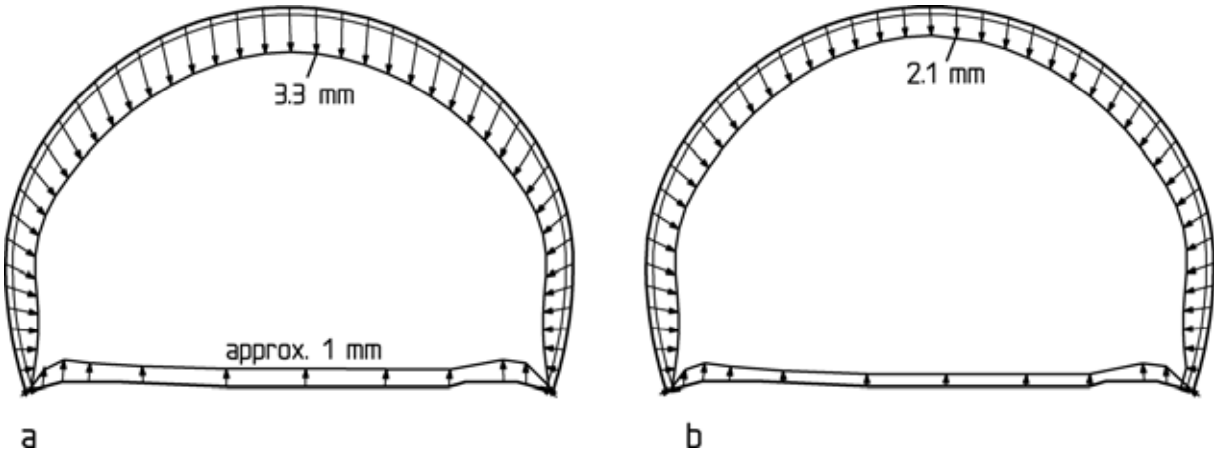

Fig. 6.39: Analysis cross-section AC 2, displacements due to full-face excavation: a) 3rd – 1st computation step; b) 3rd – 2nd computation step

Fig. 6.40 shows the stress resultants in the shotcrete membrane for the 3rd computation step. An approximate membrane state of stress is computed. The normal thrust is ranging between 400 and 1100 kN/m corresponds to only one tenth of the force resulting from the overburden. This confirms that the shotcrete membrane is only subjected to slight loading because of the high Young's modulus of the rock mass and the arching effect. The dimensioning yields that no reinforcement is statically required for the shotcrete membrane.

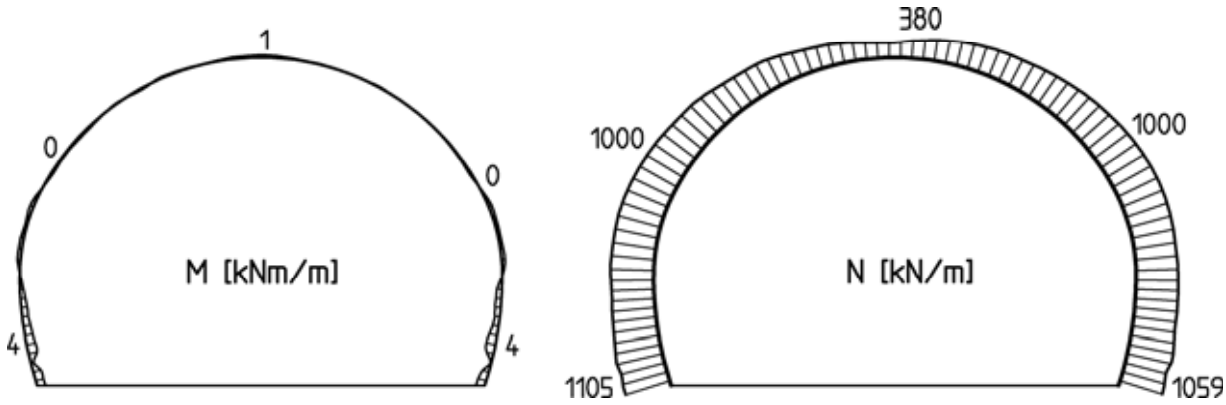

Fig. 6.40: Analysis cross-section AC 2, stress resultants in the shotcrete membrane, 3rd computation step

The excavation of the shoulders (4th and 5th computation step) does not lead to significant changes relative to the 3rd computation step.

6.2.6 Stability analyses for the design of the interior lining

Investigated load cases and load combinations

Two-dimensional FE-analyses were carried out for the design of the interior lining as well.

Fig. 6.41 shows exemplarily the FE-mesh, the boundary conditions and the parameters specified for the design of the interior lining for analysis cross-section AC 2 (see Fig. 6.26).

The computation section consists of a 1 m thick, 75 m wide and 162 m high slice subdivided into 2397 isoparametric elements with 14090 nodes.

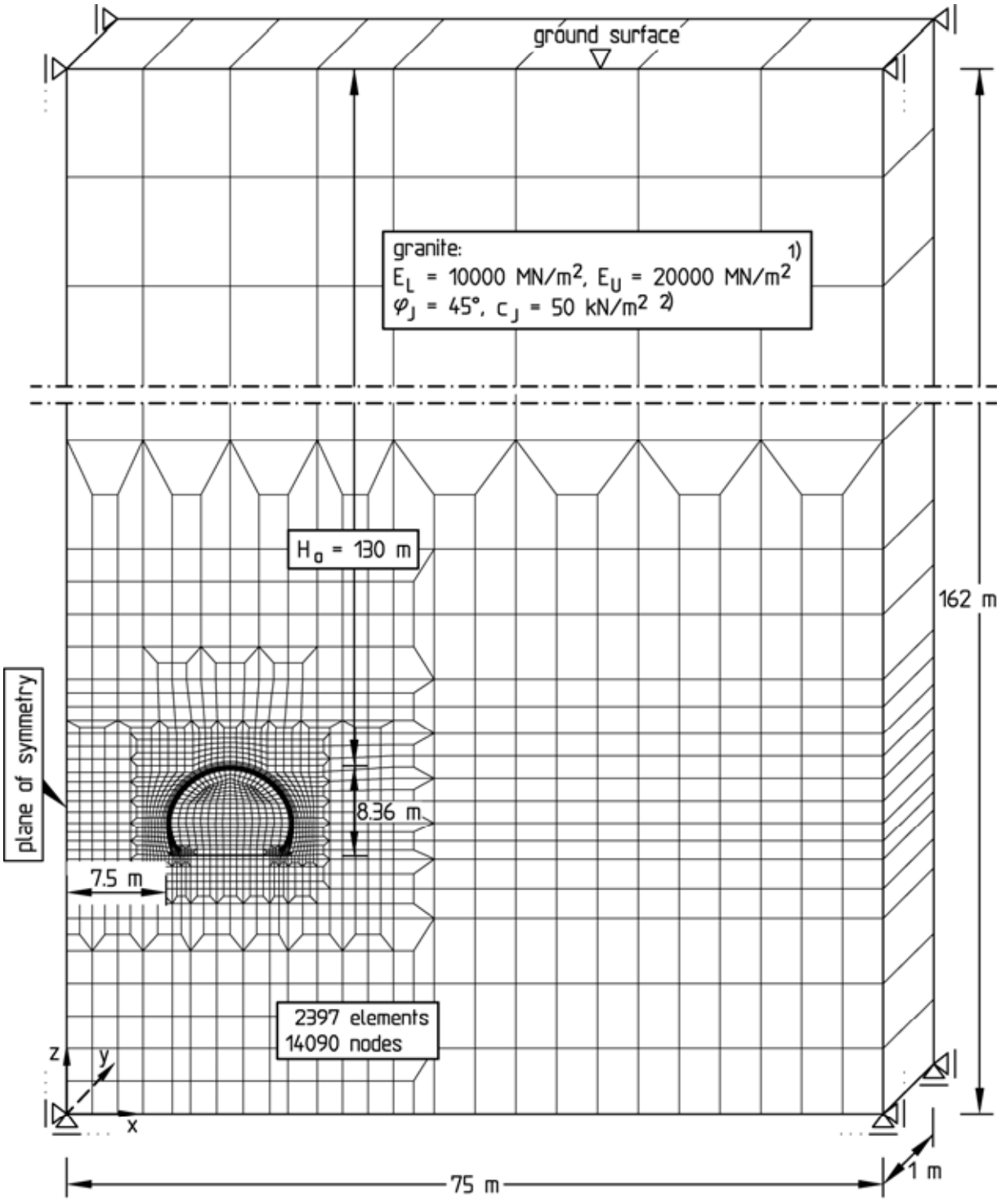

1) E_L : modulus of loading, E_U : modulus of unloading

2) J : joints with randomly distributed orientations (isotropic shear strength)

Fig. 6.41: Analysis cross-section AC 2 (interior lining), FE-mesh, boundary conditions and parameters

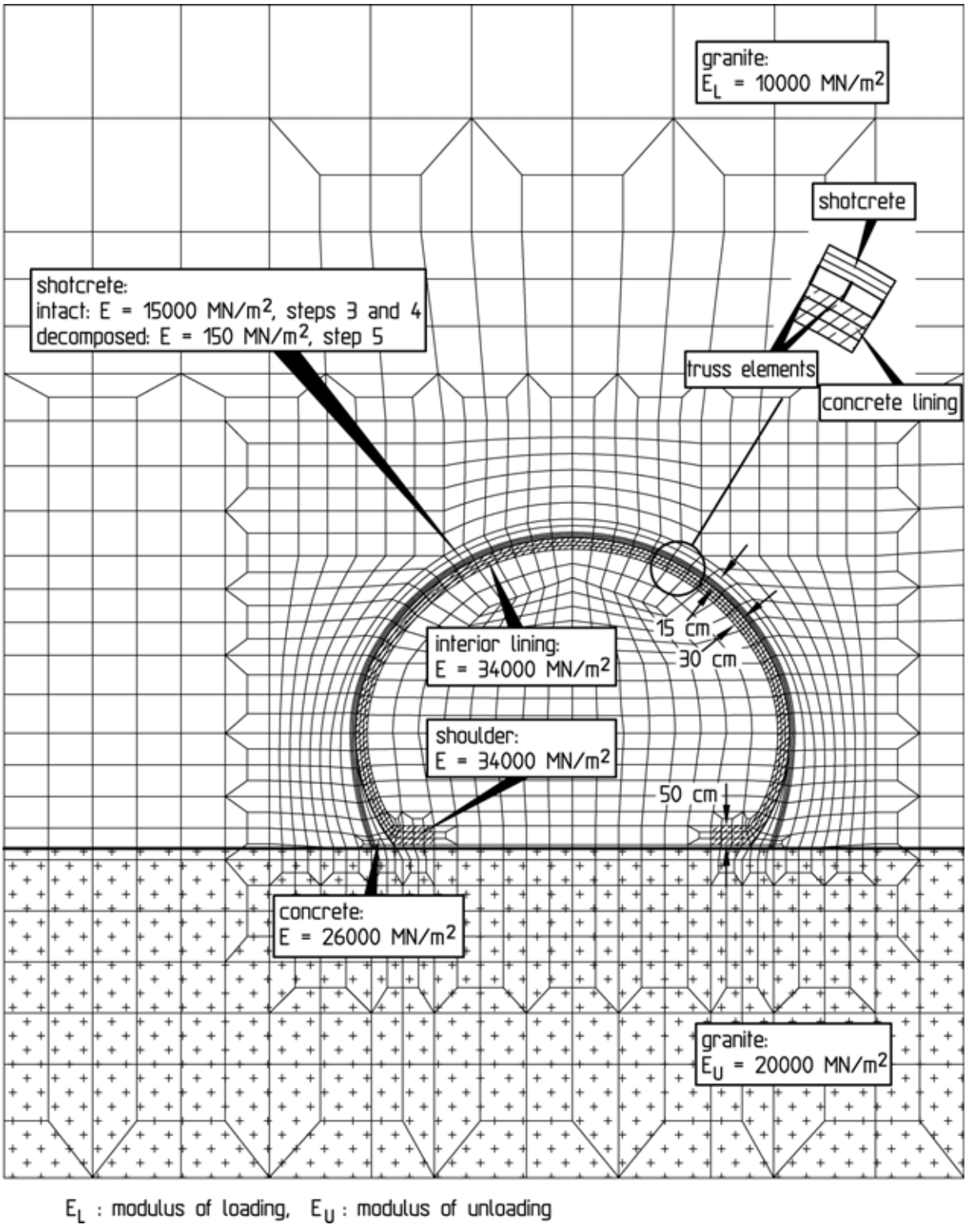

Fig. 6.42: Analysis cross-section AC 2 (interior lining), FE-mesh, detail

Unlike the stability analysis for the design of the shotcrete support, the decomposed granite and weathered granite (see Fig. 6.35) were not modeled here, since these layers are insignificant for

the loading of the interior lining. A loading modulus of E_L = 10000 MN/m^2 was assumed for the unweathered granite (Fig. 6.41 and 6.42). This value was derived from a comparison of the displacements measured during heading and the analysis results ("back-analysis", see Chapter 6.2.7).

The remaining parameters, the overburden and the specified boundary conditions correspond to those of the stability analysis for the design of the shotcrete support.

In Fig. 6.42, a detail of the FE-mesh is shown. The interior lining is modeled with a thickness of 30 cm , the shoulders with a thickness of 50 cm. The seepage water drainage is not discretized.

For the design of the interior lining it is assumed that the shotcrete will be decomposed in the course of time and lose its bearing capacity. The assumed parameters for the decomposed shotcrete are given in Fig. 6.42. Since the interior lining is only subjected to significant loads after having reached its final strength, the calculation value for Young's modulus of 34000 MN/m^2 commonly used for concrete of grade B35 is assumed (DIN 1045, 1988).

The following load cases and load combinations, respectively, were investigated for the design of the interior lining:

- Dead weight of the interior lining (DW)

- dead weight as before and rock mass pressure (DW + RP)

The seepage water is to be lowered to the invert's level by the lateral seepage water drainages (see Fig. 6.28 and 6.29). Thus there is not any water pressure acting on the interior lining, and no seepage pressure is applied to the rock mass above and closely beside the tunnel's cross-section. Such loadings are therefore not accounted for in the stability analyses for the interior lining.

The computation steps of the stability analyses for the design of the interior lining are shown in Fig. 6.43.

In the 1st computation step, the primary state in the undisturbed rock mass is computed. A preceding stress relief is simulated in the 2nd computation step with a_v = 0.5 according to (4.1).

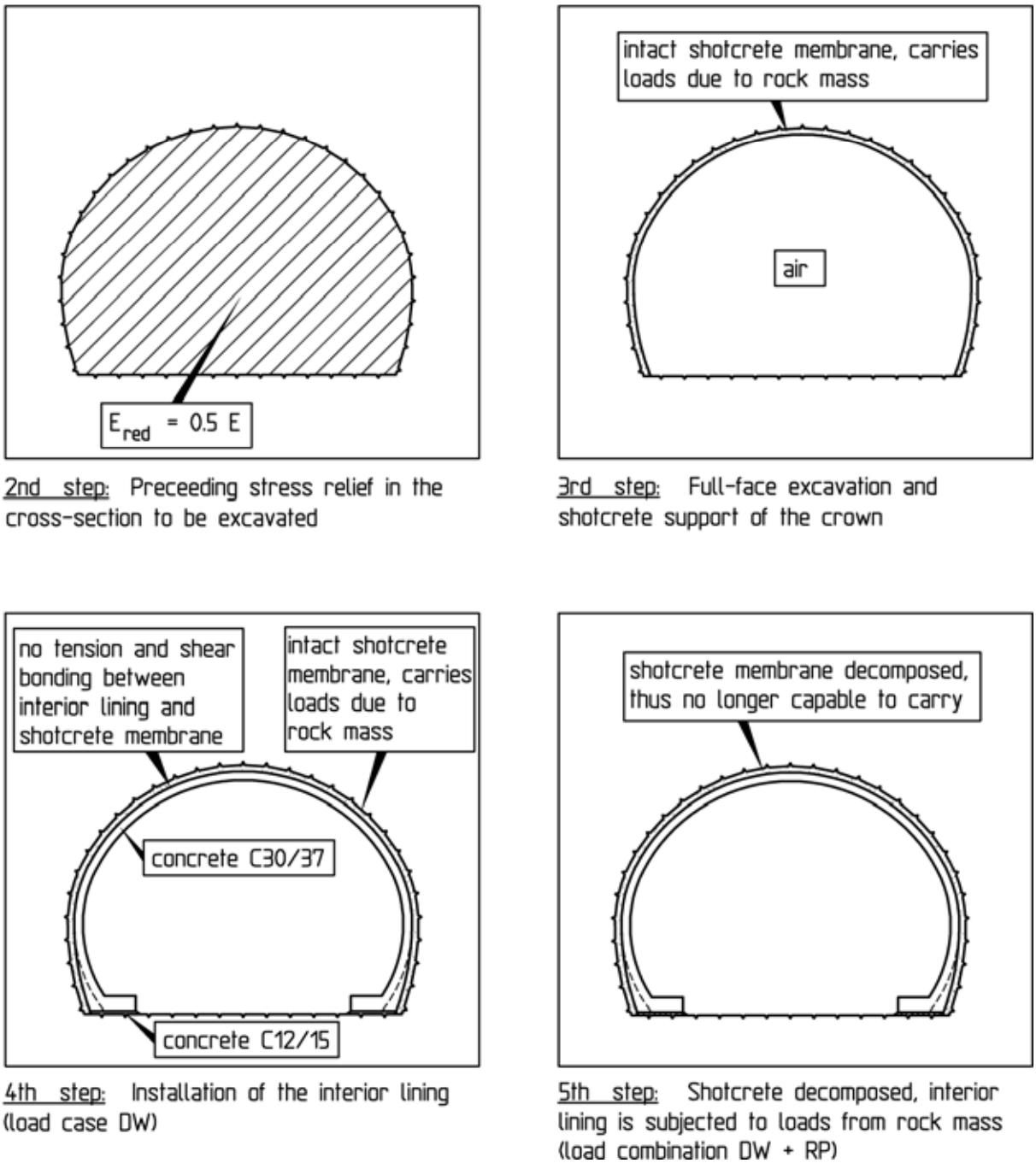

Fig. 6.43: Analysis cross-section AC 2 (interior lining), computation steps

The 3rd computation step includes the full-face excavation of the cross-section and the simultaneous installation of the shotcrete support, which carries the rock mass pressure with a Young's modulus of 15000 MN/m^2.

In the 4th computation step, the installation of the interior lining and thus load case DW is simulated. The shotcrete support is still sustainable in this state and therefore able to continue to carry the rock mass pressure. To account for the sealing between the shotcrete membrane and the interior lining, no shear and tensile forces can be transferred in computation steps 4 and 5. This is simulated by insertion of a thin row of elements between the shotcrete membrane and interior lining elements. This row of elements is assigned a stiffness of approx. zero in the 4th and 5th computation step. The opposing nodes of this element row are linked by truss elements (see Fig. 6.42), which can transfer compressive forces, but not tensile forces or shear.

In the 5th computation step, the shotcrete is assumed decomposed. As a result, the shotcrete membrane loses its bearing capacity and the interior lining must carry the rock mass pressure in addition to its dead weight.

The stress resultants of the interior lining due to dead weight (4th computation step) are shown in Fig. 6.44. If a B35 concrete grade, a lining thickness of 30 cm in the vault and 50 cm at the shoulders, a cover of the reinforcement of d_1 = 5.5 cm and safety factors according to DIN 1045 (1988) are assumed, it follows that circumferential reinforcement is not statically required. Due to the small shear forces in load case DW also a shear reinforcement is not needed.

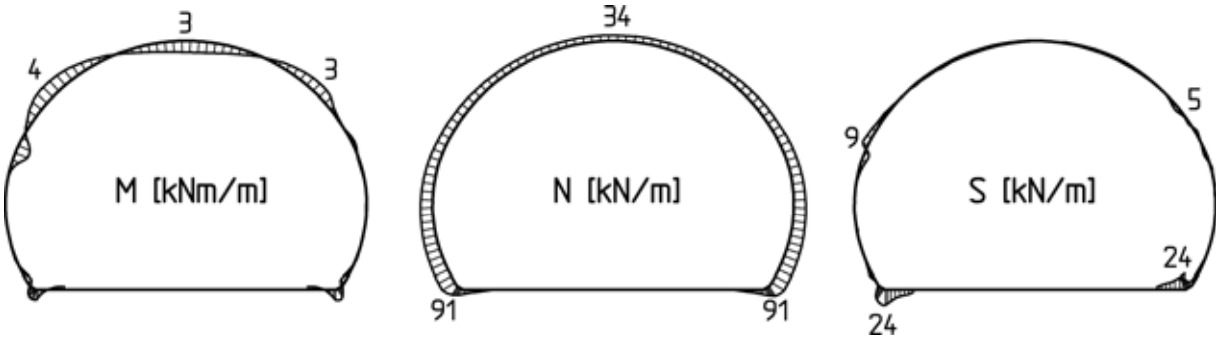

Fig. 6.44: Analysis cross-section AC 2, stress resultants in the interior lining, load case DW (4th computation step)

In the 5th computation step (load combination DW + RP) the shotcrete membrane is assumed decomposed. Stress redistributions result for this computation step compared to the preceding one. The ground carries a portion of the load previously supported by the

intact shotcrete. On the other hand, a portion of the rock mass pressure carried by the shotcrete membrane before is taken on by the interior lining. This is apparent from the increase of the stress resultants from the 4th to the 5th computation step (Fig. 6.44 and 6.45). Particularly the normal thrust in the vault and the shear force in the shoulders increase markedly as compared to the 4th computation step.

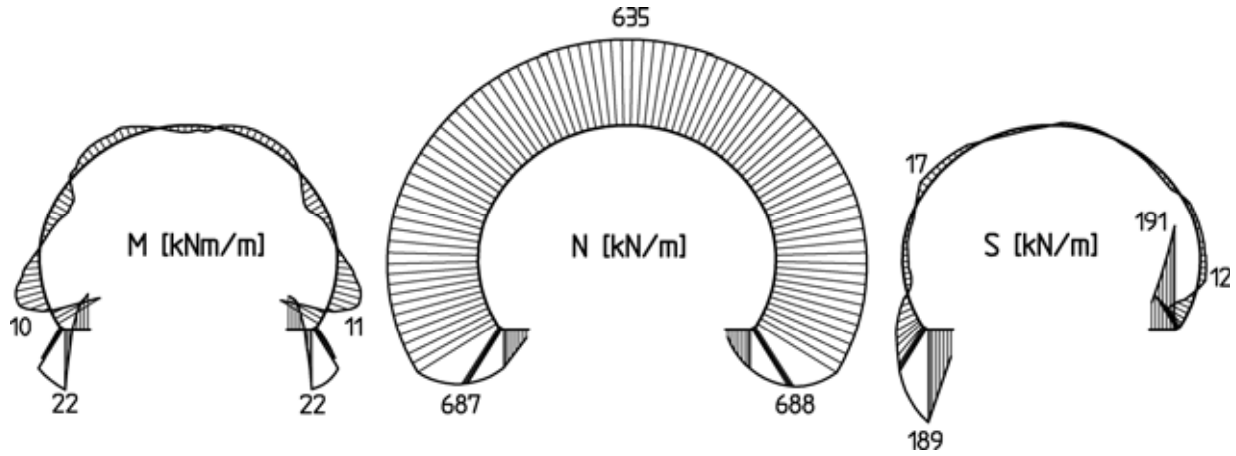

Fig. 6.45: Analysis cross-section AC 2, stress resultants in the interior lining, load combination DW+RP (5th computation step)

Vault

For the tunnel section, which is located in granite and porphyrite, the design of the interior lining yields that reinforcement is not statically required (Fig. 6.46). The interior lining was therefore constructed with plain concrete in this section. Only in the area of the special cross-sections as the breakdown bays, the cross-connections, the niches and the blockouts, a constructive reinforcement was installed (Fig. 6.47).

In the portal zones, in the weathered rock mass, in the base sediments and in the Lower Triassic sandstone a reinforcement was statically required, however.

In total, it was possible to construct the Berg Bock Tunnel over approx. 50 % of its length with an interior lining made of plain concrete.

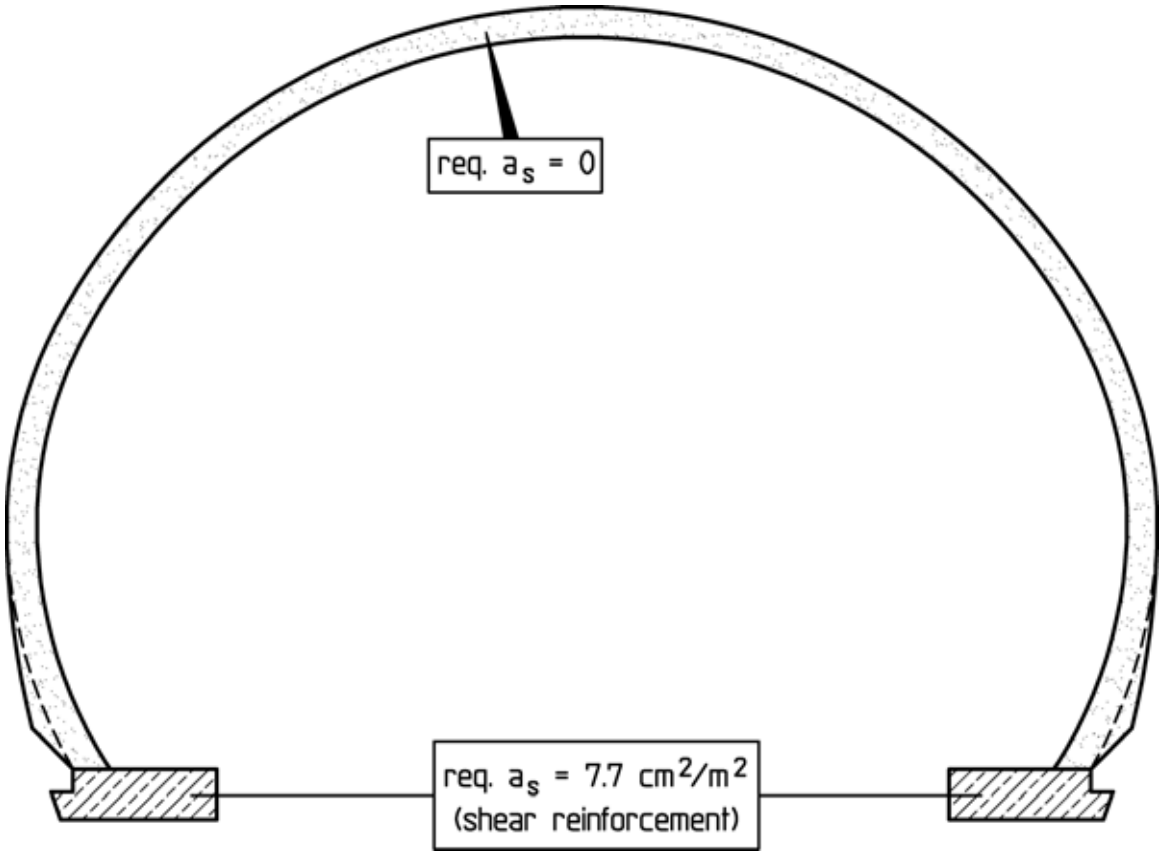

Fig. 6.46: Analysis cross-section AC 2, statically required reinforcement of the interior lining.

Fig. 6.47: Not reinforced interior lining, reinforcement in the area of a niche

Shoulders

For the shoulders, the load combination dead weight and rock mass pressure results in a required shear reinforcement of 7.7 cm^2/m^2 for analysis cross-section AC 2 (Fig. 6.46). The proof of limitation of crack width according to DIN 1045 (1988) leads to a required reinforcement for the shoulders of 12.88 cm^2/m in both, longitudinal and transverse direction. This amount of reinforcement is covered by top and bottom rebars Ø 10 mm spaced at s = 10 cm, to be placed in longitudinal and transverse direction. To cover the required shear reinforcement, steel fabric mats were bent to stirrup cages (Fig. 6.48). The shoulders were reinforced over the entire tunnel length.

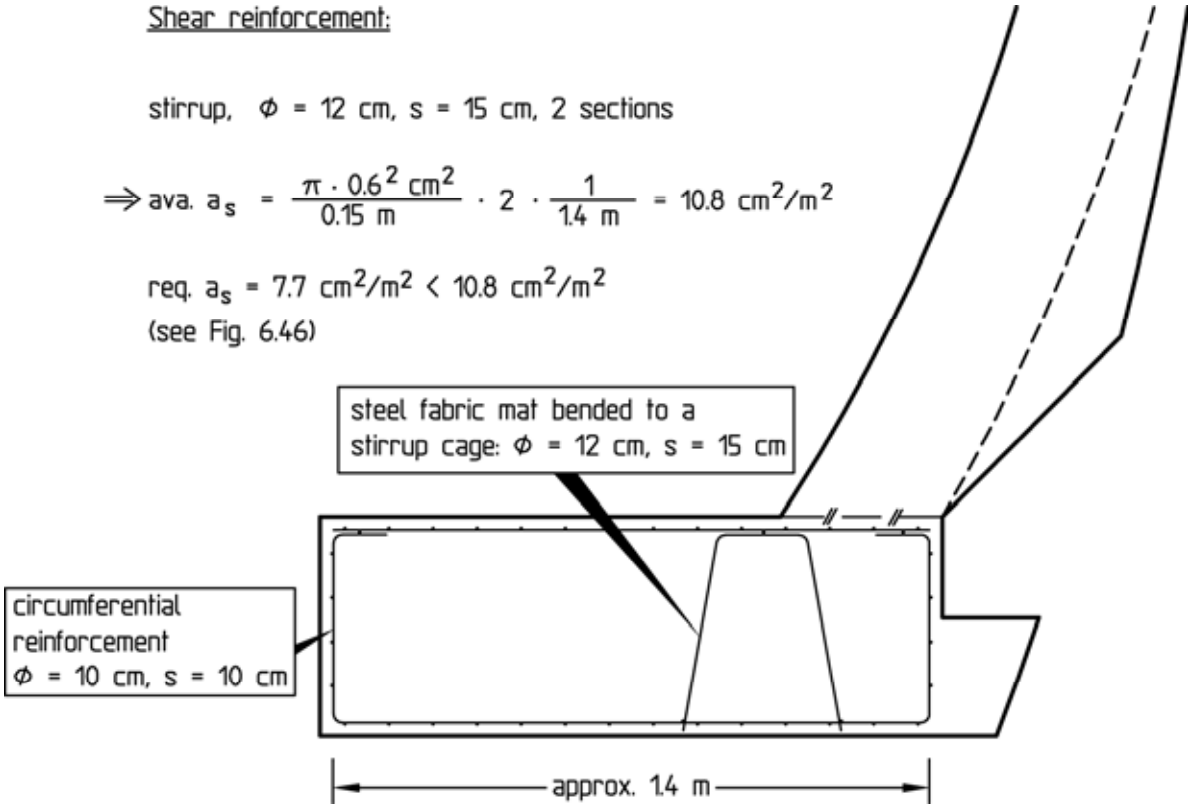

Fig. 6.48: Analysis cross-section AC 2, reinforcement of the shoulders

6.2.7 Monitoring

The heading of the Berg Bock Tunnel was accompanied by a geotechnical monitoring program.

In the longitudinal section of Fig. 6.49 the range of the roof subsidence measured after the heading of the entire tunnel was completed is exemplarily shown.

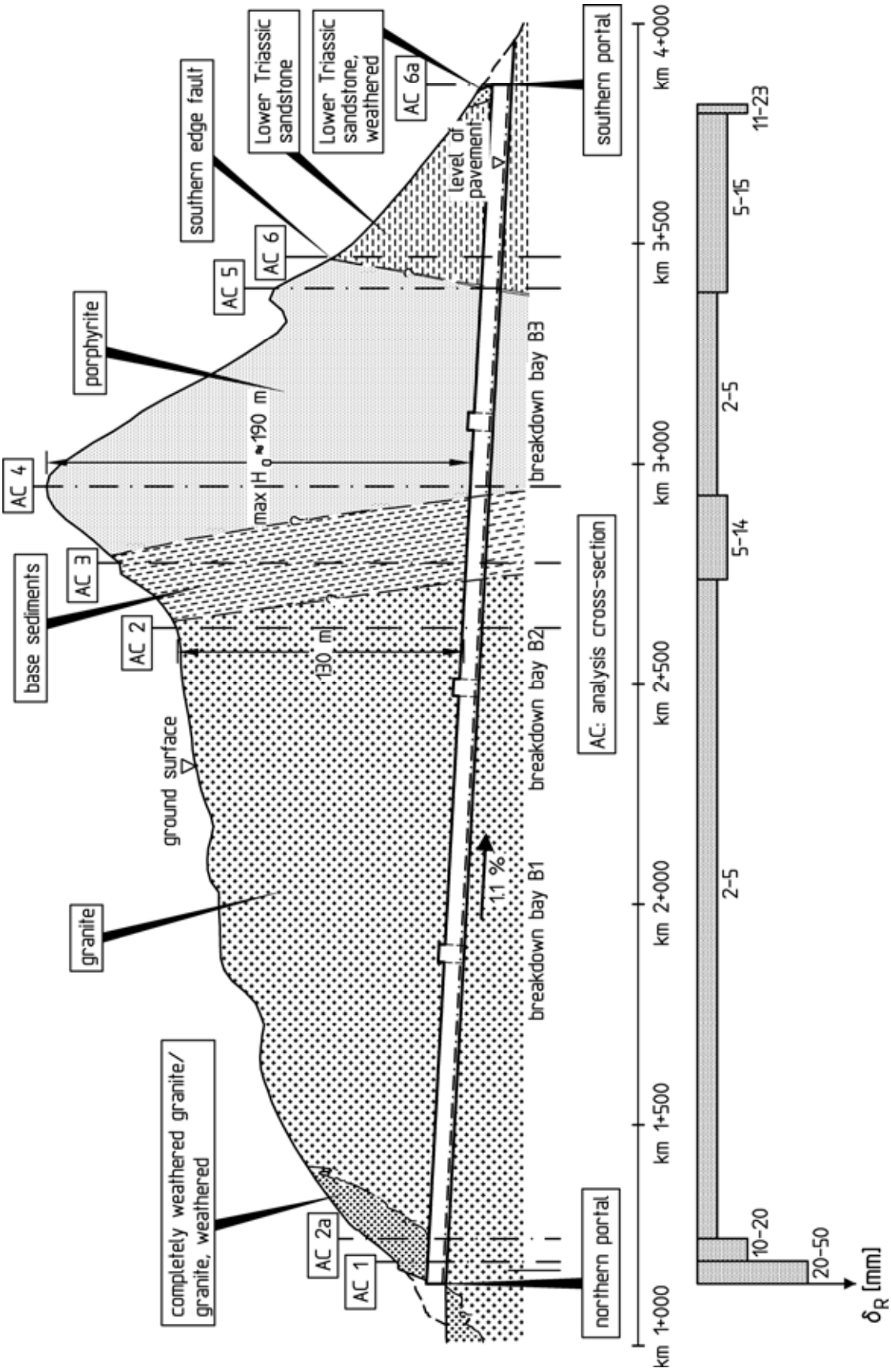

Fig. 6.49: Range of measured roof subsidence δ_R, longitudinal section

The largest subsidence was measured in the portal areas with values between 10 and 50 mm. In those tunnel sections where the cross-section is located in granite or porphyrite, a roof subsidence between 2 and 5 mm was measured. In the base sediments and in the Lower Triassic sandstone the roof subsidence ranges from 5 to 15 mm.

As an approximation, the measurements captured only those displacements that occurred after the installation of the shotcrete membrane. Therefore, the measurement results in the granite area must be compared to the computed displacements shown in Fig. 6.39b (3^{rd} – 2^{nd} computation step). A roof subsidence of approx. 2 mm was computed. This analysis is based on a loading modulus of the unweathered granite of E_L = 15000 MN/m^2 (see Fig. 6.35). A comparative analysis with E_L = 10000 MN/m^2 yields a roof subsidence of approx. 4 mm. It is thus possible to reproduce the roof subsidence measured in the granite and the porphyrite well in the analyses using a loading modulus of approx. 10000 MN/m^2 (see Fig. 6.49). This value was therefore taken as a basis for the stability analyses of the interior lining.

6.2.8 Conclusions

The Berg Bock Tunnel is situated in granite and porphyrite over a length of 2 × 2000 m corresponding to 75 % of its total length. In these sections, the tunnel was headed by full-face excavation using the drill and blast method with comparatively great round lengths and limited support measures.

Due to the low deformability and the high strength of the rock mass, the ground was able to carry approx. 90 % of the overburden load, and the means of support only had a slightly assisting function. On this basis it was possible to optimize the heading conception and to excavate both tunnel tubes in a very short time. With the construction of the interior lining using plain concrete over approx. 50 % of the total tunnel length, the costs for the interior lining could be kept low as well.

An important tool for the optimization of the heading and the means of support were the FE-analyses. Their results were confirmed by the experience made and the monitoring during the excavation.